Reaction Kinetics and TTT Cure Diagrams for Off-Stoichiometric Ratios of a High-T_g Epoxy/Amine System

S. L. SIMON and J. K. GILLHAM*

Polymer Materials Program, Chemical Engineering Department, Princeton University, Princeton, New Jersey 08544

SYNOPSIS

The cure behavior of two off-stoichiometric ratios, one amine-rich and the other epoxy-rich, of a high-T_g aromatic difunctional epoxy/aromatic tetrafunctional diamine system are studied using differential scanning calorimetry (DSC). The curing reactions are presumed to consist of competing epoxy/amine reactions and a subsequent reaction of epoxy with hydroxyl, termed etherification, that is significant in the epoxy-rich system after depletion of amino hydrogens. A one-to-one relationship between conversion and T_g independent of cure temperature is found for each of the off-stoichiometric systems in spite of the competing reactions. Since it is uniquely related to fractional conversion, sensitive, and easily measured, T_g is used to monitor the curing reactions. Kinetically controlled master curves for isothermal cure are obtained for each system by shifting T_g vs. ln time data to an arbitrary reference temperature; apparent activation energies for the epoxy/amine and the etherification reaction regimes appear to be identical at 15.5 kcal/mol. Experimental DSC data are satisfactorily described for both systems by a kinetic model of the competitive epoxy/amine and etherification reactions. The ratio of the rate constants for the reactions of epoxy with the secondary amine group and epoxy with the primary amine group, $\alpha = k_2/k_1$, is found to be approximately 0.5 (i.e., equal reactivity of amino hydrogens), whereas the ratio of the rate constants for the reactions of epoxy with hydroxyl and epoxy with the primary amine group, $\beta = k_3/k_1$, is found to be 0.001. Diffusion control is incorporated in the model by the use of a free-volume theory. Vitrification and iso-T_g contours in the time–temperature–transformation (TTT) isothermal-cure diagram are calculated for both systems from the kinetic model. © 1992 John Wiley & Sons, Inc.

INTRODUCTION

Understanding the cure of thermosetting systems is important to their use in structural composite, adhesive, coating, reaction injection molding, and electronic applications. The isothermal time–temperature–transformation (TTT) cure diagram, adapted to polymers[1,2] and shown in Figure 1, is a useful intellectual framework for analyzing and designing cure processes. The diagram displays the time to reach various events during isothermal cure vs. cure temperature, T_c. As a thermosetting material cures, its glass transition temperature, T_g, increases from an initial value of T_{g0} due to increasing molecular weight, which occurs with a corresponding decrease in the fraction of free volume associated with chain ends (e.g., unreacted epoxy and primary amine groups in the presently investigated systems). Molecular gelation is the incipient formation of infinite molecules that occurs, for the simplest systems, at a specific conversion and a corresponding T_g of ${}_{gel}T_g$. After gelation, T_g increases due to increasing cross-link density, as well as to increasing number-average molecular weight (of the sol/gel mixture) and to the decrease in chain ends. As T_g approaches the temperature of cure, the material enters the glass transition region and is defined to vitrify when T_g equals T_c. At the particular cure temperature of ${}_{gel}T_g$, the material will gel and vitrify simultaneously. The segmental mobility is substan-

* To whom correspondence should be addressed.

Journal of Applied Polymer Science, Vol. 46, 1245–1270 (1992)
 CCC 0021-8995/92/071245-26

tially decreased in the vicinity of the glass transition, and the overall rate of the reaction may become progressively controlled after vitrification by the limiting diffusion of reacting species.[3,4] The reaction rate in this regime is affected by both chemical and physical aging: The molecular mobility decreases with increasing conversion due to increasing departure from physical equilibrium (e.g., $T_g - T_c$); and the mobility decreases with time due to physical aging which occurs when the material is in the nonequilibrium state below its glass transition. If the cure temperature is above the T_g of the fully cured material, $T_{g\infty}$ by definition, the material cannot vitrify at T_c; in this case, the chemical kinetics governs the progress of the reaction.[3,4]

The TTT isothermal cure diagram is based on the phenomenological changes that take place during cure, such as vitrification and macroscopic gelation, the latter of which can correspond operationally, e.g., to the attainment of a definite viscosity. The diagram has been expanded to include other contours, specifically ideal molecular gelation, vitrification, and iso-conversion or iso-T_g curves, which can be calculated both in the kinetic- and diffusion-controlled regimes if a complete kinetic model of the reaction is known.[3,4]

There are three principal curing reactions considered to occur in epoxy/amine systems[5-19]: the reaction of epoxy with primary and secondary amines, and the anionic polymerization reaction of epoxy with hydroxyl generated in the epoxy/amine reactions. The reaction between epoxy and hydroxyl is also referred to in the literature as homopolymerization or polyetherification. Because of the stoichiometry and the step-growth mechanism which are involved, however, it is considered that the reaction is terminated after the first step so that etherification, rather than polyetherification, is of importance in this work. The reactions considered are thus:

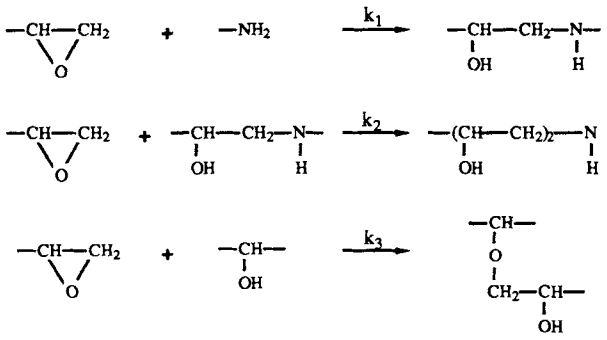

Kinetic mechanisms for the reactions have been reviewed in the literature.[5,6]

Although much work has been published on the cure kinetics of epoxy/amine systems, there is disagreement in the literature concerning the magnitude of the rate constants of the considered reactions. The value of the ratio of the rate constants for the reaction of epoxy with the secondary and

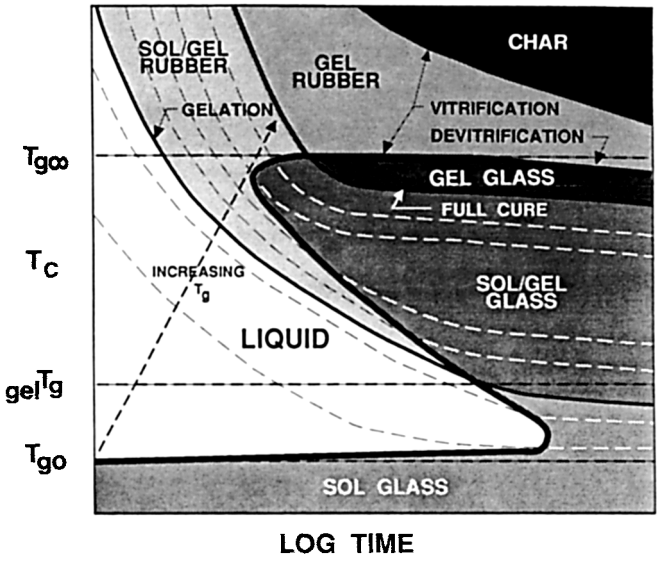

Figure 1 Generalized TTT isothermal cure diagram. Reproduced with permission from *Journal of Applied Polymer Science,* Vol. 41, No. 11, pp. 2885–2929 (1990).

primary aromatic amine groups, $\alpha = k_2/k_1$, is generally reported to be temperature-independent and to range from 0.1 to 0.5,[6–15] where the value of 0.5 corresponds to equal reactivity of amino hydrogens. (A value of 1 is expected for equal reactivity if the reaction model is written in terms of primary and secondary amino hydrogen atoms rather than of primary and secondary amine groups since the concentration of primary amino hydrogen atoms is twice that of primary amine groups.) The value of α is generally determined by one of two methods: (1) the use of a kinetic reaction model (with α as a parameter) to fit the experimental rate data or to predict a relation between the concentrations of reactant and product species; and (2) the determination of the critical stoichiometric ratio of epoxy to amine (with amine in excess) necessary for incipient gelation at 100% reaction of epoxide. Discrepancies in the value of α obtained by the various methods and for various epoxy/amine systems can be attributed to various factors, including the following: When using a reaction model, errors include oversimplification of the kinetic model or use of experimental data after the onset of diffusion control when the kinetically controlled reaction model is no longer applicable; when determining α from the critical stoichiometric ratio for gelation, errors may arise from intramolecular reactions (particularly internal etherification prevalent in diglycidylaniline-type epoxies where the epoxy groups are in close proximity); and from nonhomogeneities in the network.[7,8] Further, the sensitivity of various techniques for measuring reactant or product concentrations or for measuring incipient molecular gelation can lead to erroneous results. For example, it was found in one study in our laboratory that fitting of DSC rate data over a wide range of temperatures could be accomplished assuming that the ratio $\alpha = k_2/k_1 = 0.5$.[3,4] However, in another study on the same system, using Fourier transform infrared spectroscopy (FTIR) and fitting the data to a relation derived from the same reaction model, it was observed that the value of k_2/k_1 varied with temperature from 0.16 at 100°C to 0.33 at 160°C.[9] However, the accuracy of the FTIR fractional conversion data is at best ± 0.02, and since determination of the ratio required fitting the data at high conversions of primary amine, the error in the ratio is considered by the present authors to be at least ± 0.1. In other laboratories, discrepancies have also been observed in the values of k_2/k_1 obtained by different methods.[10]

The etherification reaction of epoxy with hydroxyl is found to be much slower than the addition of epoxy and amine[5,16,17] and, consequently, has been found in other work to occur at a measurable rate in excess epoxy systems only after essentially all amino hydrogens are depleted[7,8,16,18] and at temperatures above 150°C.[7,8,11] Etherification is considered to be catalyzed by strong tertiary amines and other bases.[19] However, kinetic models of the epoxy/amine polymerization reactions that have incorporated etherification have generally not considered catalysis of the etherification reaction by the tertiary amine, presumably because of steric hindrance. In any case, the predictions of a kinetic model incorporating etherification will not be affected by not explicitly incorporating tertiary amine catalysis because its concentration will be constant (all amino hydrogens will be depleted) when the rate of etherification becomes significant. Literature data have been analyzed to obtain the rate constants for a kinetic model describing the reaction of a tetrafunctional aromatic epoxy (tetraglycidyl methylene dianiline) cured with diaminodiphenyl sulfone (DDS) system in epoxy-rich stoichiometric ratios (1 : 0.35 to 1 : 0.50).[11] In that work, one of the systems for which data were analyzed was cationically catalyzed with $BF_3 : NH_2C_2H_5$, whereas another was a commercial mixture that presumably contained catalytic impurities, and, hence, the results may not be applicable to the system investigated here. The rate of etherification was assumed to be first order with respect to both epoxy and hydroxyl, and the ratio of the rate constants for the etherification reaction to the reaction of epoxy with the primary amine group was found to range from 0.1 to 0.5, increasing with increasing temperature, for the various data analyzed.[11] In work by other researchers on a system without cationic catalyst, a difunctional aromatic epoxy (diglycidyl aniline) cured with a stoichiometric amount of DDS, the etherification reaction has been assumed to proceed by two mechanisms, one uncatalyzed and the other catalyzed by hydroxyl, and the ratio of the rate constants for uncatalyzed etherification and the uncatalyzed reaction of epoxy with primary amine, as well as the ratio for both catalyzed reactions, ranged from 0.01 to 0.05, increasing with increasing temperature.[14] The discrepancy in the ratios of the rate constants obtained in the two works is probably because the former work analyzed systems that were cationically catalyzed.

The model of a reaction should be able to describe the reaction throughout the whole range of cure, taking into account diffusion control, which for this system is particularly observable for the epoxy/amine reactions after vitrification. To this end, the rate of the reaction is generally considered to be the reciprocal of the sum of the time scale for the ki-

netically controlled chemical reaction plus the time scale for diffusion, with the latter time scale increasing with conversion.[3,4,20,21] Consequently, in the early stages of cure, the rate constant is dominated by the kinetic rate constant, whereas at higher conversions and after vitrification, it is dominated by the diffusion rate constant. Various empirical equations can be used to describe the dependence of the diffusion rate constant on temperature, for example, by using the inverse relationship between viscosity and diffusivity. The Williams–Landel–Ferry (WLF) equation ($\eta/\eta_{T_g} = C_1(T - T_g)/(C_2 + T - T_g)$, where η is viscosity, η_{T_g} is the viscosity at T_g, and C_1 and C_2 are constants)[22] and the Doolittle free volume equation ($\eta = A \exp(b/f)$, where f is free volume and A and b are constants)[23] are equilibrium equations, generally considered valid from T_g to approximately 50°C above T_g. These equations qualitatively predict the large decrease in the mobility observed upon vitrification, but with the WLF "universal" parameters predict that the mobility will be zero approximately 52°C below T_g. The modified WLF equation [$\eta/\eta_{T_g} = C_1(T - T_g)/(C_2 + |T - T_g|)$],[24] which was used in our laboratory to model the time scale of diffusion in the glass transition region below T_g for the 1 : 1 stoichiometric ratio of the system studied in this work,[3,4] is qualitatively more correct in the glassy state as it predicts a leveling off of the mobility in this region. However, since it has been shown that the relaxation rate of iso-free-volume materials in the glassy state is dependent on temperature, the Macedo and Litovitz equation, in which free volume and temperature are independent parameters, may better describe the diffusivity directly below T_g [$\eta = A \exp(b/f) \times \exp(-E/RT)$, where E is the activation energy for molecular mobility].[25] The latter equation was used to model the extent of reaction after vitrification and to model related properties vs. conversion for a cyclic aliphatic amine/epoxy system.[20] None of these equations takes into account the nonequilibrium nature of the glass below T_g so that physical aging effects cannot be taken into consideration. An approach derived from more basic nonequilibrium thermodynamic principles does incorporate the effect of physical aging on the diffusivity.[21] The average relaxation time, τ, is determined from the Adam and Gibbs equation [$\ln \tau = C + \Delta\mu s^*/RTS$, where $\Delta\mu$ is the energy barrier to configurational change for the smallest cooperative region with an entropy s^*, $S = \Delta C_p \ln (T/T_2)$, ΔC_p is the change in heat capacity at T_g, T_2 is the temperature at which the equilibrium configurational entropy is zero, and C is a constant] and is equated to the diffusion time scale that is used to determine the diffusion-controlled reaction rate constant.[21]

Previous work in our laboratory modeled the kinetics of the 1 : 1 stoichiometric ratio of an aromatic difunctional epoxy/aromatic tetrafunctional diamine system.[3,4] The model, with parameters obtained from isothermal differential scanning calorimetry (DSC) experiments successfully described experimental isothermal data throughout the complete range of cure, in the kinetically controlled region prior to vitrification and in the diffusion-controlled regime after vitrification, as well as the results of temperature-scanning experiments.[26] The assumption of equal reactivity of amino hydrogens was used and the rate equation was assumed to be second-order autocatalytic (third order overall) in form.

In the present work, the curing reactions are investigated for both an amine-rich mixture and an epoxy-rich mixture of the aromatic epoxy/aromatic diamine system, the 1 : 1 stoichiometric ratio of which was studied earlier. T_g is used as a direct measure of conversion. Time–temperature superposition of T_g vs. ln time DSC data yields a kinetically controlled master curve, as well as the apparent activation energy of the polymerization reactions. A kinetic model of the reactions, incorporating etherification and diffusion-control, is used to describe the data in both kinetically controlled and diffusion-controlled regimes. Using the kinetic model, iso-T_g contours as well as the vitrification curve of the TTT isothermal cure diagram are calculated for each system. A preliminary report on this work has been published.[27] A more complete report is available.[28]

MATERIALS

The chemical system used is a liquid difunctional epoxy (diglycidyl ether of bisphenol A, DER 332, Dow Chemical Co., with an equivalent epoxy molecular weight of 174 g/eq; theory = 170 g/eq) cured with a pure tetrafunctional aromatic diamine (trimethylene glycol di-*p*-aminobenzoate, TMAB, Polaroid Corp., with a theoretical equivalent amino hydrogen molecular weight of 78.5 g/eq). The chemical structures of the reacting materials are shown in Figure 2. Two off-stoichiometric ratios of the reactants are studied: an excess amine mixture (1 : 1.2 epoxy groups to amino hydrogen atoms) and an excess epoxy mixture (1 : 0.8 epoxy groups to amino hydrogen atoms). Master batches of approximately 5 g of each stoichiometric ratio are mixed at 100°C in vials placed in a heated oil bath with

CHEMICAL REACTANTS

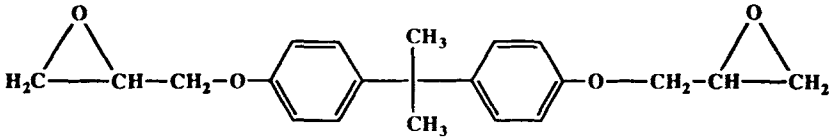

Diglycidyl Ether of Bis-phenol A

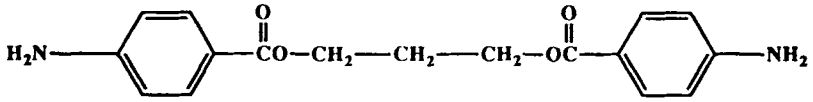

Trimethylene Glycol Di-p-aminobenzoate

Figure 2 Chemical structures of the reactants.

the crystalline amine (melting point = 125°C) added slowly to the hot liquid epoxy. The mixtures are stirred with an electric stirrer until the solutions become clear and homogeneous: 30 min for the excess amine sample and 15 min for the excess epoxy sample. (To achieve homogeneity, the more viscous amine-rich mixture required stirring for a longer time than for either the epoxy-rich or 1 : 1[3,4] mixtures, the latter two of which were both stirred for 15 min.) The warm mixtures are subsequently degassed in a vacuum oven at room temperature for 15 min and poured into aluminum pans. The pans are put into zip-lock plastic bags, which are placed in a desiccator and put in the freezer for storage (≈ -15°C). This procedure is consistent with that used previously for the 1 : 1 stoichiometric sample in order to make valid comparisons between the three systems of different stoichiometry.[3,4] Minimal reaction occurs during the initial mixing process: The conversion of the uncured samples is found to be less than 2% by titration experiments carried out by Dow Chemical Co.,[29] and calculations based on the proposed model, see later, predict 0.3 and 0.6% conversion during the mixing process for the epoxy-rich and amine-rich systems, respectively. The glass transition temperatures of the uncured mixtures, T_{g0}, are -4 ± 1 and -9 ± 1°C for the amine-rich and epoxy-rich stoichiometries, respectively, as compared to a value of −5°C reported for the 1 : 1 mixture.[3,4]

EXPERIMENTAL

All experimental data reported in this work were obtained from differential scanning calorimetry (DSC) studies using a Perkin-Elmer DSC-4 unit. Ten to fifteen milligram samples of uncured resin are "sealed" in aluminum DSC pans and cured in the preheated DSC unit at isothermal cure temperatures from 100 to 200°C for various cure times ranging from 10 min to 24 h. The cured samples are then cooled at 10°C/min to −30°C and subsequently scanned during heating at 10°C/min to 350°C. For isothermal times longer than 24 h, samples are cured in a press oven at the same cure temperatures for 1–7 days, with a sample of each stoichiometry being removed each day, free-cooled and placed in the DSC furnace at room temperature. These samples are then quenched to −30°C and then scanned to 350°C at 10°C/min. (No discontinuity in the data is observed between the DSC-cured and the oven-cured data.) Samples that had vitrified during isothermal cure ($T_g > T_c$) show an endothermic physical aging peak in the vicinity of T_g.[3,4,28] To eliminate the physical aging peak, and therefore the effects of physical aging on T_g, these samples are quenched to −30°C at 320°C/min after scanning at 10°C/min to just beyond the physical aging peak and then rescanned to 350°C at 10°C/min. (In retrospect the quench rate should have been 10°C/min for all cooling.) Minimal reaction is considered to occur in

the first scan to just beyond the physical aging peak based on two observations: (1) the apparent T_g of the aged material from the first scan is always greater than the T_g from the second scan since the relaxation times are longer in the aged material; (2) using the kinetic model equations that describe the reaction (see later), the increase in T_g due to the temperature scan to erase the physical aging peak is found to be less than 1°C.[28]

DSC scans at 10°C/min show an endothermic step-change in heat capacity at the glass transition; T_g is taken as the midpoint of this transition. The DSC temperature scan also yields the heat flow from the sample as it reacts at temperatures above T_g.

The basic assumption underlying the use of the DSC technique is that the heat flow measured is proportional to the reaction rate or, after integration, that the total heat evolved during the DSC scan is proportional to the heat evolved by the reaction during the run. This infers that the change in the rubber (or liquid) heat capacity, if any, with increasing conversion does not significantly affect the results. This assumption is reasonable.[28]

On preliminary scans to 380°C of uncured material, shown in Figure 3(a) and (b) for the amine-rich and epoxy-rich systems, respectively, one principal exotherm is observed corresponding to the reactions of epoxy with the primary and secondary amines, with a maximum rate of heat evolution at 218°C for the amine-rich system and 225°C for the epoxy-rich system. Hereafter, this exotherm will be referred to as the epoxy/amine exotherm. A second exotherm of the epoxy-rich system is observed in Figure 3(b) with a maximum at approximately 370°C. This second exotherm is complicated by the onset of degradation reactions that occur in the vicinity of 380°C in the temperature scan (and are often characterized by erratic endothermic and exothermic spikes and noise in the data). In the amine-rich system, this second exotherm does not occur: Only the epoxy/amine exotherm and the onset of degradation reactions at approximately 380°C are observed. The 1 : 1 stoichiometric system also does not display the second exotherm.[3,4] Since the second exotherm occurs only in the epoxy-rich system, it is considered that it represents reaction of the excess epoxy. In other reported work, an exothermic DSC peak observed between 300 and 380°C during temperature-scanning experiments for various cured epoxy resins was attributed by FTIR studies to isomerization and/or etherification of unreacted epoxide.[30] The kinetic model (see later), which satisfactorily describes the epoxy/amine and etherification reactions at the isothermal cure temperatures investigated ($\leq$ 200°C), predicts a reaction rate significantly less than that observed in the DSC temperature scans above 320°C. It is consequently supposed that a reaction involving excess epoxy with a higher activation energy than the etherification reaction, possibly isomerization, is partially responsible for the second exotherm observed in the temperature scans of the epoxy-rich system.

The residual heat of the epoxy/amine reactions is estimated by drawing a straight line connecting the base line before and after the epoxy/amine exothermic peak and integrating the area under the peak. Since the second exotherm due to reaction of excess epoxy in the epoxy-rich system overlaps the epoxy/amine exotherm, the base line of the DSC trace will appear to slope downward.[31] The apparent heat of the epoxy/amine exotherm will be overestimated if the base line is assumed to be horizontal with a vertical boundary. If a linear sloping base line is used, as was the case for this work, the heat of the epoxy/amine exotherm will be underestimated and are corrected for as below).

The total heat of the epoxy/amine reactions is obtained by scanning an initially uncured sample. For the amine-rich system, the total heat of the epoxy/amine reactions is -25.8 ± 1.4 kcal/mol of reacting epoxy (based on five trials) assuming that all of the epoxy reacts and accounting for the excess amine. For the epoxy-rich system, the total (underestimated) heat of the first exotherm due to the epoxy/amine reactions is -21.9 ± 1.7 kcal/mol of reacting epoxy (based on 15 trials) assuming that the stoichiometric amount of epoxy (80%) reacts with all of the amine and adjusted to account for the excess epoxy. The total heat of epoxy/amine reactions in the 1 : 1 stoichiometric mixture was reported to be -23.0 kcal/mol of the reacting epoxy.[3,4]

It is expected that the actual normalized total heat (per gram of reacting epoxy) for the epoxy/amine exotherm will be the same for all stoichiometries if the heats of the reactions of epoxy with primary amine hydrogens and secondary amine hydrogens are equal and if the exotherm is due only to the epoxy/amine reactions. The observed normalized total heats for the epoxy/amine exotherm appear to decrease with increasing epoxy concentration: -25.8 ± 1.4, -23.0, and -21.9 ± 1.7 kcal/mol of reacting epoxy (for the amine-rich, 1 : 1, and epoxy-rich systems, respectively). However, the total heat of the epoxy/amine exotherm for the epoxy-rich system is underestimated due to the sloping base

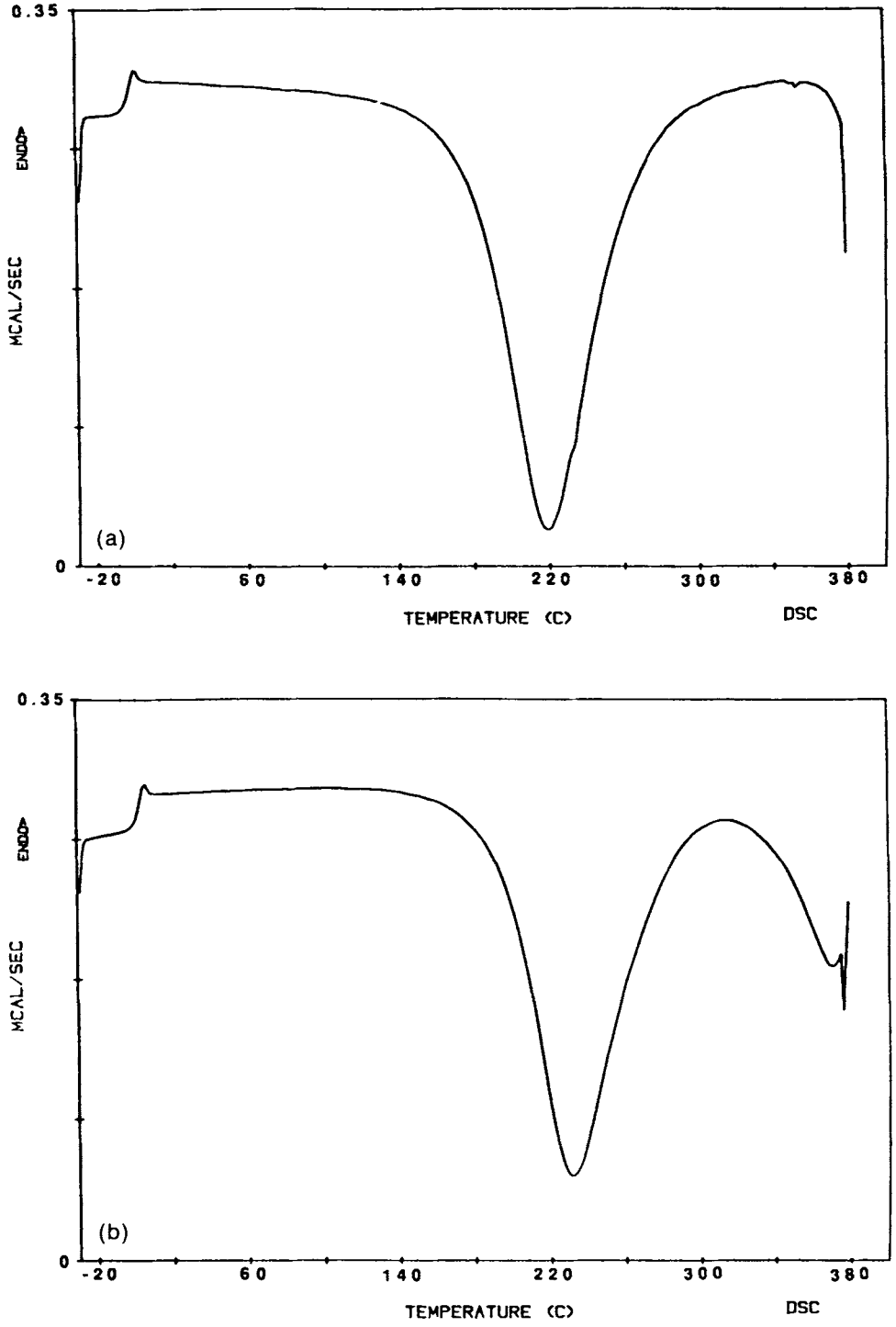

Figure 3 (a) DSC scan of amine-rich sample, initially uncured, from −30 to 380°C at 10°C/min showing T_g, the exotherm for the epoxy/amine reactions, and the onset of degradation at approximately 380°C. (b) DSC scan of epoxy-rich sample, initially uncured, from −30 to 380°C at 10°C/min showing T_g, the exotherm for the epoxy/amine reactions, the exotherm of excess epoxy reactions, and the onset of degradation at approximately 380°C.

line caused by the reactions of excess epoxy. Consequently, it is assumed that the change in total heat with stoichiometry is an experimental artifact.

The error in the total heat of the epoxy-rich system (i.e., for the unreacted system) due to the sloping base line is approximately 10%, assuming that the actual heat of the epoxy/amine reactions is approximately 24.4 kcal/mol of epoxy, the average of the total heats for the amine-rich and 1 : 1 systems. (In retrospect, it may have been more appropriate to use the amine-rich total heat as the actual value.) However, the percent error will increase as the residual heat decreases due to the apparent sloping base line, with the experimentally observed residual heat appearing to be zero prior to full completion of the epoxy/amine reactions.[28] Consequently, the underestimated residual heats for the epoxy-rich system are corrected by assuming a linear relationship between the actual and underestimated heats.[28] The correction is not large but is significant at high conversions: The corrected conversion is 96% of the uncorrected conversion (underestimated heats yield overestimated conversions).[28] All further conversion data reported for the epoxy/amine reaction in the epoxy-rich system are corrected.

The conversion of a partially cured sample is proportional to the heat evolved during cure prior to the DSC temperature scan assuming that the heat of reaction does not change with extent of reaction. The heat evolved during cure is assumed to be the total heat evolved for an uncured sample minus the residual heat evolved during the DSC scan. The fractional conversion of the limiting reactant, $x_{\text{limiting reactant}}$, due only to the epoxy/amine reactions, can thus be calculated from the residual heat of the epoxy/amine exotherm for the partially cured specimen, ΔH_{r1}, and the total heat of the epoxy/amine exotherm for the uncured material, ΔH_{T1}, with both heats being corrected for the sloping base line in the epoxy-rich system. Assuming that the epoxy/amine reactions go to full conversion of the limiting reactant:

$$x_{\text{limiting reactant}} \text{ (due to epoxy/amine reactions)} = \frac{\Delta H_{T1} - \Delta H_{r1}}{\Delta H_{T1}} \quad (1)$$

For the amine-rich system, the limiting reactant is epoxy. It is assumed that the only significant reactions occurring in the amine-rich system are between epoxy and amine and that all of the epoxy reacts. Consequently, the fractional conversion of epoxy, x, is equal to the fractional conversion of the limiting reactant due to epoxy/amine reactions:

$$x = 1 - \frac{\Delta H_{r1}}{\Delta H_{T1}} \quad (2)$$

where the conversion of epoxy is

$$x = \frac{e_0 - e}{e_0} \quad (3)$$

where e_0 and e are the initial concentration of epoxy and the concentration of epoxy, respectively. In the case where etherification occurs, the conversion of epoxy due only to the epoxy/amine reactions is multiplied by the fraction of epoxy that will react with amine, which for the epoxy-rich system is the reciprocal stoichiometric ratio r ($= e_0/2a_{10}$, where a_{10} is the initial concentration of primary amine):

$$x \text{ (due to epoxy/amine reactions)} = \frac{1}{r}\left(1 - \frac{\Delta H_{r1}}{\Delta H_{T1}}\right) = 0.8\left(1 - \frac{\Delta H_{r1}}{\Delta H_{T1}}\right) \quad (4)$$

The total conversion of epoxy is the conversion due to the epoxy/amine reactions plus that due to the etherification reaction. The DSC dynamic temperature scan at 10°C/min is not suitable for measuring the residual heat of the reaction of the excess epoxy in the epoxy-rich system since there is competition with degradation reactions, as shown in Figure 3(b). Even at the slowest scanning rates investigated, 1 and 2°C/min, the second exotherm is still complicated by degradation.[28] The residual heat of the reaction of excess epoxy can, however, be measured isothermally at 320°C in less than 60 min after completion of the epoxy-amine reactions by a scan to 320°C. The isothermal hold at 320°C, shown in Figure 4(a) and (b) for an amine-rich and an epoxy-rich sample, respectively, shows that an exotherm is observed only for the epoxy-rich sample. It is assumed that this exotherm at 320°C is due to reactions of the excess epoxy. At the isothermal cure temperatures investigated ($\leq$ 200°C), the only significant reaction of the excess epoxy is considered to be etherification that can go to completion in the time scale studied (the residual heat of the isothermal exotherm at 320°C decreases to zero and T_g plateaus at the T_g of the fully cured material, $T_{g\infty 2}$ [see later]), whereas at the temperature of the isothermal exotherm, 320°C, both etherification and isomerization are presumed to occur. The total heat of the isothermal exotherm at 320°C for an initially uncured epoxy-rich sample is -20 ± 3 kcal/mol of

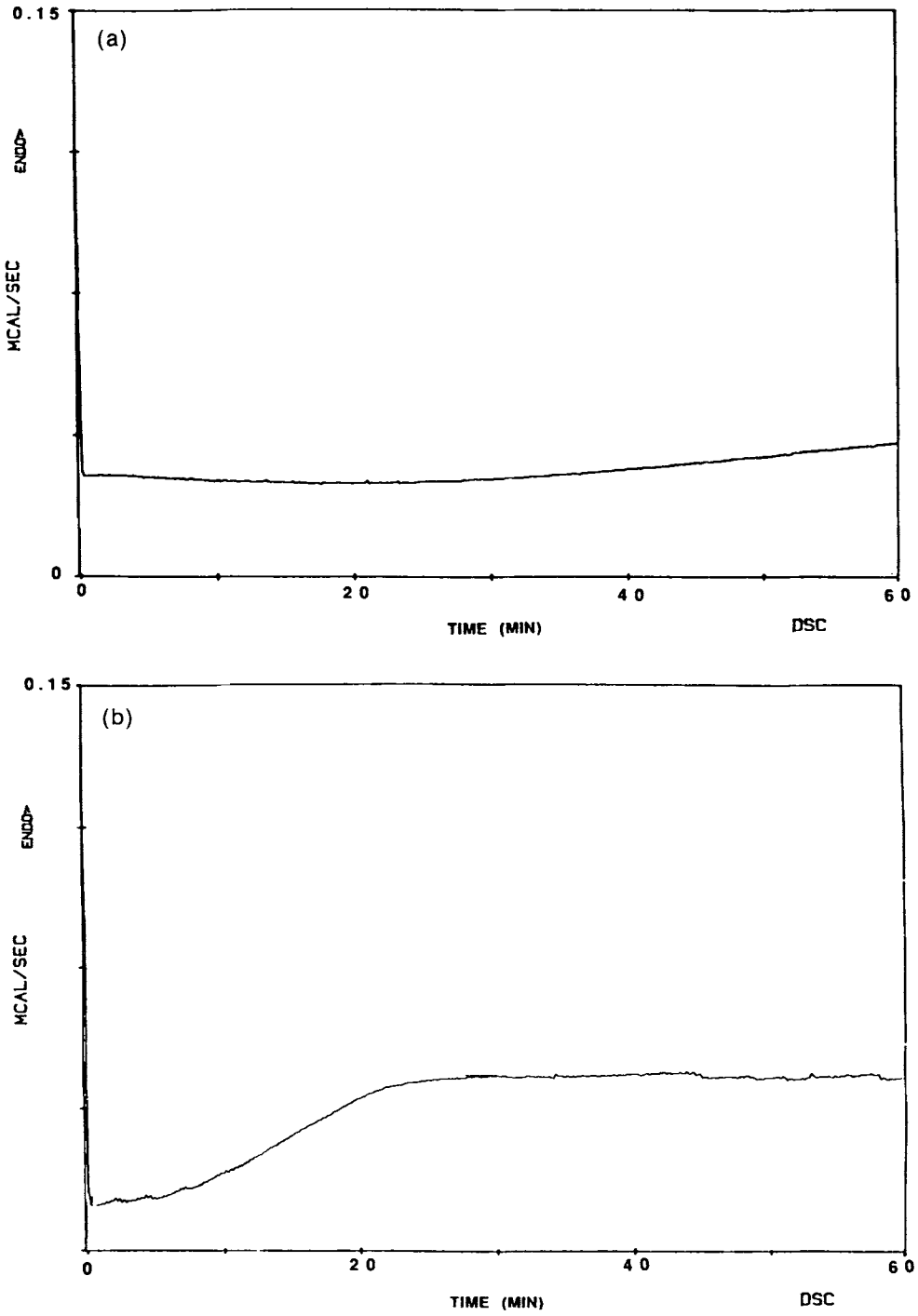

Figure 4 (a) DSC isothermal hold at 320°C for initially uncured amine-rich sample, after scanning from −30 to 320°C at 10°C/min, indicating no heat evolved. (b) DSC isothermal hold at 320°C for initially uncured epoxy-rich sample, after scanning from −30 to 320°C at 10°C/min, showing exotherm of excess epoxy reactions.

reacting epoxy. This value for the heat of the reactions of excess epoxy is slightly lower than the value for the heat of the reaction of epoxy with amine (≈ -24.4 kcal/mol of reacting epoxy), as would be expected based on the results and calculations of other researchers.[32]

The residual heat of the excess epoxy reactions at 320°C is assumed to be proportional to the un-

reacted excess epoxy and, thus, is related to the conversion of etherification that occurred at the isothermal cure temperatures ($T_c \leq 200°C$). Note that since the ratio of the isothermal exotherm at 320°C for a partially cured sample relative to that of the total heat at 320°C for an uncured sample is used [see eq. (5)], no error is introduced by having the DSC calibrated at 10°C/min. The following DSC scanning program is used to investigate the reaction of excess epoxy: −30 to 320°C at 10°C/min followed by a hold at 320°C for 60 min. This ramp/hold program will be referred to as Method 2, in contrast to the previously described ramp to 350°C, which will be termed Method 1. From the ramp/hold schedule of Method 2 for a partially cured epoxy-rich sample, the T_g of the partially cured material, the residual heat of the epoxy-amine reactions, and the residual heat of the reactions of the excess epoxy are obtained. The conversion due only to the etherification reaction is determined from the residual heat of the isothermal exotherm at 320°C, whereas the conversion due to the epoxy/amine reactions is determined from the residual heat of the epoxy/amine exotherm in the temperature scan. It is assumed that any etherification that occurs during the epoxy/amine exotherm is balanced by reaction of epoxy with amine that occurs during the isothermal exotherm and vice versa.[28]

Visual inspection of samples show no physical evidence of char formation or gas evolution during the isothermal hold at 320°C. The scatter of the conversion vs. T_g data obtained by the ramp/hold Method 2 (in Fig. 6 for $x \gtrsim 0.8$), however, is considered to be due to degradation reactions occurring during the isothermal exotherm at 320°C, even though for the data presented no erratic peaks or noise was observed in the DSC traces. However, weight loss on the order of 1% is found by weighing DSC samples before and after scanning. This weight loss and any endothermic heat associated with it is neglected, as well as any enthalpic change produced by degradation reactions during the isothermal hold at 320°C. Consequently, the residual heat obtained by the isothermal exotherm of Method 2 is considered to be less accurate than that obtained for the epoxy/amine exotherm during the temperature scan. However, a calculated T_g vs. conversion relationship will be used when modeling the kinetics of the reaction to transform T_g to conversion. The DSC data in the etherification regime are used only to show their consistency with the calculated curve.

The total fractional conversion of epoxy, x, for the epoxy-rich system is equal to the fraction that has reacted with amine plus the fraction that has reacted by etherification at the cure temperature ($\leq 200°C$) and can be calculated from the corrected residual heats of a partially cured specimen for the epoxy/amine reactions, ΔH_{r1}, and for the reaction of excess epoxy, ΔH_{r2}, using the total heats of each of these reactions for the uncured material, ΔH_{T1} and ΔH_{T2}, respectively, and assuming that the reactions go to completion. It is assumed that during cure ($T_c \leq 200°C$) the amine reacts with the stoichiometric amount of epoxy (80%), whereas the excess epoxy (20%) reacts by etherification:

$$x = 1 - \frac{1}{r}\frac{\Delta H_{r1}}{\Delta H_{T1}} - \left(1 - \frac{1}{r}\right)\frac{\Delta H_{r2}}{\Delta H_{T2}}$$

$$= 1 - 0.8\frac{\Delta H_{r1}}{\Delta H_{T1}} - 0.2\frac{\Delta H_{r2}}{\Delta H_{T2}} \qquad (5)$$

For samples that were scanned to 350°C (Method 1), only ΔH_{r1} is obtained. The value of ΔH_{r2} is estimated by a calibration plot of ΔH_{r1} vs. ΔH_{r2} from the data obtained by Method 2.[28]

RESULTS AND DISCUSSION

T_g vs. Conversion Relationship

Other work on epoxy/amine systems has shown that there is a unique one-to-one relationship between T_g and conversion independent of cure temperature,[3,4,12,26,32–37] and in work from this laboratory, T_g has also been used as a measure of conversion to study the kinetics of the stoichiometric 1 : 1 ratio of the systems investigated in this work.[3,4] The T_g vs. conversion relationship for the amine-rich system also appears to be unique and independent of cure temperature for those temperatures studied, as shown in Figure 5. For the epoxy-rich system, the relationship is also unique and independent of cure temperature for conversions below 0.8, as shown in Figure 6. Data at higher conversions show more scatter, and, consequently, the uniqueness of the relationship in this regime is not proved although it is expected since the activation energies of the various reactions are similar and the reactions are essentially sequential (see later). In Figure 6 for the epoxy-rich system, the larger symbols refer to data obtained by measuring only the first exotherm (Method 1), whereas the smaller symbols refer to data obtained from the ramp/hold DSC program where both the exotherms due to epoxy/amine and excess epoxy reactions were measured (Method 2).

T_g is a more accurate and sensitive parameter for

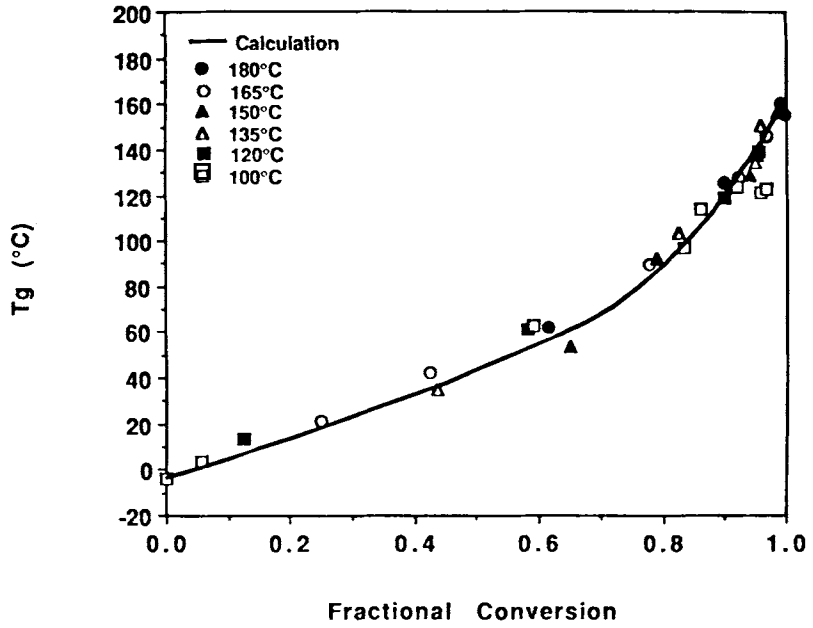

Figure 5 One-to-one relationship between T_g and epoxy conversion, x, for the amine-rich system. The full line is the calculation using eq. (6) with constants $k = 0.00175e_0$, $K = 0.24$, and $\Psi = 0.0$.

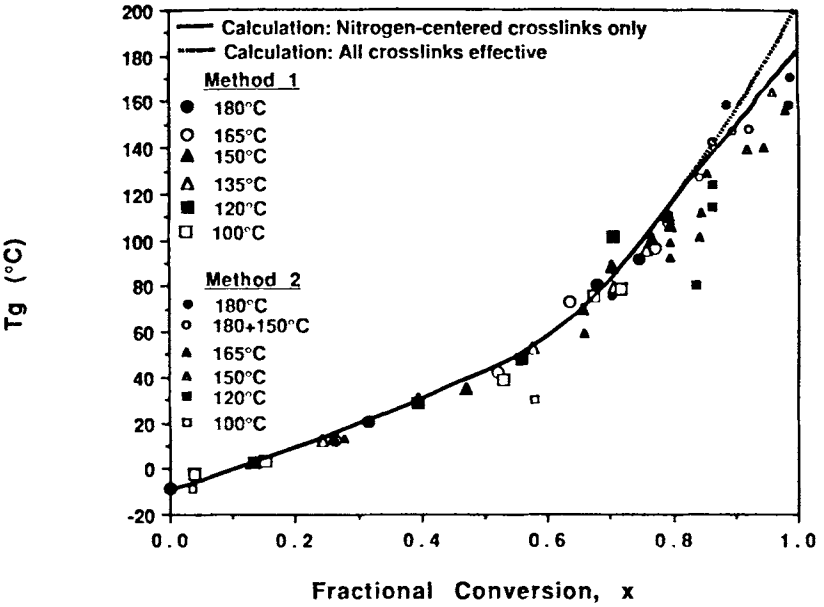

Figure 6 One-to-one relationship between T_g and epoxy conversion, x, for the epoxy-rich system. Large symbols are data obtained by DSC Method 1; smaller symbols are data obtained by DSC Method 2. The full line is the calculation using eq. (6) considering that only nitrogen-centered cross-links are effective, whereas the dotted line is obtained if all cross-links are considered equally effective. The constants used for both calculations are $k = 0.00175e_0$, $K = 0.24$, and $\Psi = 0.0$.

monitoring the reaction than is conversion calculated from the residual heat of reaction.[3,4,33] T_g varies over a large range ($\geq 170°C$ from T_{g0} to $T_{g\infty}$ for the systems studied), and it is easily and sensitively measurable by DSC (to approximately $\pm 1°C$). Comparatively, the errors in the residual heat measurement are considerably higher ($\pm 8\%$ for the total heat of the epoxy/amine reactions and $\pm 15\%$ for the excess epoxy reactions). The nonlinear, upward curving relationship between T_g and conversion also makes T_g a more sensitive measure of reaction in the later stages of cure. For the etherification reaction, following T_g rather than conversion determined from residual heat allows the reaction to be studied rather easily. Consequently, T_g is the primary variable used in this work. When epoxide conversion is needed, e.g., to model the kinetics of the reaction, T_g values are transformed to conversion using a theoretical fit of the one-to-one T_g vs. conversion relationship as described below, which reduces the error associated with the experimental data.

It is of interest to examine the physical basis of the T_g vs. conversion relationship, as well as to describe it mathematically using an equation based on theoretical considerations. The empirical DiBenedetto equation, which has been given a theoretical basis,[38] has been used to successfully describe the experimental T_g vs. conversion data for the 1 : 1 system studied earlier in this laboratory.[2,26] However, the DiBenedetto equation is essentially a one-parameter model, with the parameter dictating the curvature of the relationship. Consequently, it is not able to describe the data of the epoxy-rich system, in which consecutive reactions change the nature of the cross-links such that the T_g vs. conversion relationship changes at a conversion of approximately 0.8 (Fig. 6). To describe the present data, the effects of network parameters are examined below, and an equation recently published[32] is adapted.

The one-to-one relationship between T_g and conversion implies that either the molecular structure of the materials cured at different cure temperatures is the same (i.e., if the reactions of epoxy with primary amine, secondary amine, and hydroxyl have similar activation energies) or that the difference in molecular structure for materials cured at different temperatures does not have a significant effect on the glass transition temperature (i.e., the differences in structure occur on a size scale smaller than that measured by T_g). One study in this laboratory indicated that the ratio k_2/k_1 for the 1 : 1 stoichiometric mixture of the epoxy/amine system of this work does vary with cure temperature[9] (as discussed). Because of that result, a theoretical model was developed to demonstrate that T_g is not dependent on the relative rates of reaction of primary and secondary amines.[36] In that model, each amine group was considered to be a trifunctional cross-link point if its arms are infinite, i.e., trifunctional because the two diamine groups in the tetrafunctional diamine curing agent are separated by a segment whose length is on the order of the epoxy monomer.[3,4,36] Using such a definition of the cross-link point, it was shown that the cross-link density as well as the number-average molecular weight of the sol before gelation and of the sol/gel mixture after gelation are not strong functions of the ratio k_2/k_1. By considering T_g to be a function of cross-link density and number-average molecular weight, both of which are insensitive to the ratio k_2/k_1, and neglecting the effect of changes in polarity, T_g was shown to be insensitive to the ratio of the rates of the two competing epoxy/amine reactions.[36]

It has been shown that for linear polymers, T_g is related to the number-average molecular weight,[39] with T_g increasing with increasing number-average molecular weight because of decreasing configurational entropy. T_g is also affected by the concentration of dangling chain ends, which tend to decrease T_g due to the increase in configurational entropy associated with the free ends. In a linear polymer, the concentration of dangling chain ends is inversely proportional to molecular weight in the absence of intramolecular reactions; hence, the theoretical relationship for T_g vs. conversion needs to include only one parameter. In previous work from our laboratory, the number-average molecular weight of the sol, and of the sol/gel mixture after gelation, was used in the expression for T_g for thermosetting systems.[3,4,36,37] In these systems, the reciprocal number-average molecular weight is a weak second-order function of chain-end concentration in the absence of intramolecular reactions, which can be approximated by a linear relationship.[28] However, in the presence of intramolecular reactions, which occur particularly after gelation, the molecular weight is not linearly related to chain-end concentration, so that using molecular weight as the independent variable will not adequately account for the rise in T_g with conversion due to disappearance of chain ends in the gel. Consequently, a better approach may be to use the concentration of chain ends (i.e., conversion) as the independent variable rather than number-average molecular weight.

A recently developed equation is used in this work to describe T_g as a function of cross-link density and conversion[32]:

$$T_g(x) = T_{gu}(x)\left(\frac{1}{1-\frac{KX}{1-\Psi X^2}}\right)$$

$$= \left(\frac{1}{\frac{1}{T_{g0}} - kx}\right)\left(\frac{1}{1-\frac{KX}{1-\Psi X^2}}\right) \quad (6)$$

where $T_{gu}(x)$ is the glass transition temperature of the uncross-linked but branched system at an epoxide fractional conversion x (hypothetical after gelation), T_{g0} is the initial glass transition temperature of the unreacted material, and X is the cross-link density. The constants k, K, and Ψ incorporate the effects of chain ends, cross-links, and non-Gaussian behavior of segments at high cross-link density, respectively. The constant K has been shown by analysis of experimental data for various systems to vary for segments of different chemical structure, but is expected, along with Ψ, not to vary with stoichiometry.[32] Obviously, however, in the epoxy-rich system where different reactions form different chemical structures, the effectiveness of different cross-links may vary. To account for this in this work, K is considered constant and the cross-link density X is taken as the effective cross-link density. (In the amine-rich system, where only the epoxy/amine reactions occur, the effective cross-link density will be the actual cross-link density, whereas in the epoxy-rich system, the effective cross-link density will not necessarily be the actual cross-link density, as described later.) The constant k implicitly incorporates the effect of branching (which increases T_g) and explicitly incorporates the plasticization effect of chain ends (which decreases T_g). The constant k is expected to vary with stoichiometry according to the present work, being proportional to e_0 if the increase in T_g due to the reaction of the primary amino hydrogen is the same as the increase due to the reaction of the secondary amino hydrogen.[28]

The cross-link density, X, is determined by employing the recursive technique of Miller and Macosko (in which the recursive nature of the branching process and elementary probability laws are used to calculate properties such as cross-link density and molecular weight as functions of conversion).[40] Equal reactivity of amino hydrogens is assumed and is consistent with the findings of this work (see later). The recursive method could also be applied to the case where $\alpha = k_2/k_1 \neq 0.5$; however, the cross-link density would not be significantly affected.[36] For the amine-rich system, in which only the epoxy/amine reactions are assumed to occur, the density of trifunctional cross-links is (using the notation of the previous authors[40])

$$X = \frac{a_{10}}{2}(4P(F_A^{out})[1 - P(F_A^{out})]^3 + 2[1 - P(F_A^{out})]^4) \quad (7)$$

$$P(F_A^{out}) = \left(\frac{1}{x_B x_A} - \frac{3}{4}\right)^{0.5} - \frac{1}{2} \quad (8)$$

where a_{10} is the initial concentration of primary amine groups, $P(F_A^{out})$ is the probability that looking out from A leads to a finite chain rather than to the infinite network, and x_i is the fractional conversion of i (= A or B), where A is the amino hydrogen and B is the epoxy moiety. The probability of finding a finite chain lies between 0 (corresponding to full conversion for the 1 : 1 stoichiometric system where $x_A = x_B = 1$) and 1 (corresponding to molecular gelation). Prior to molecular gelation, the probability of finding an infinite chain is zero, as is the cross-link density.

For the epoxy-rich system, the recursive method is used to determine the cross-link density, but in contrast to the amine-rich system, the hydroxyl groups, C, generated in the epoxy/amine reactions are allowed to react with epoxy. The following equations, based on the schematic shown, can be solved to obtain the probabilities of finding a finite rather than infinite chain on looking out of A, $P(F_A^{out})$; into B, $P(F_B^{in})$; out of B, $P(F_B^{out})$; into C, $P(F_C^{in})$; out of C, $P(F_C^{out})$; and into A, $P(F_A^{in})$:

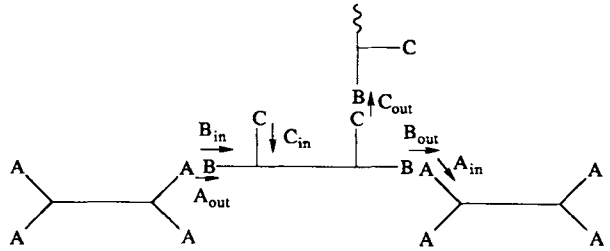

$$P(F_A^{out}) = x_A P(F_B^{in}) + 1 - x_A \quad (9)$$

$$P(F_B^{in}) = [x_{B,A}P(F_A^{in}) + x_{B,C}P(F_C^{in})]P(F_C^{out})^2$$

$$+ (1 - x_B)P(F_C^{out}) \quad (10)$$

$$P(F_B^{out}) = x_{B,A}P(F_A^{in}) + x_{B,C}P(F_C^{in}) + 1 - x_B \quad (11)$$

$$P(F_C^{in}) = \frac{[x_{B,A}P(F_A^{in}) + x_{B,C}P(F_C^{in})]}{x_B} \times \{[x_{B,A}P(F_A^{in}) + x_{B,C}P(F_C^{in})]P(F_C^{out}) + 1 - x_B\} \quad (12)$$

$$P(F_C^{out}) = x_C P(F_B^{in}) + 1 - x_C \quad (13)$$

$$P(F_A^{in}) = P(F_A^{out})^3 \quad (14)$$

where $x_{B,A}$ and $x_{B,C}$ are the fractional conversions of epoxy, B, due to reaction with amino hydrogen and hydroxyl, A and C, respectively, and x_C is the fractional conversion of hydroxyl ($= [Et]/(e_0 - e) = x_{B,C}/x_B$, where $[Et]$ is the concentration of ether linkages). Using the above relationships, equations for $P(F_B^{in})$ and $P(F_C^{in})$ are obtained that are solved simultaneously by reiterative techniques for the roots between 0 and 1. Once $P(F_B^{in})$ and $P(F_C^{in})$ are found, the other probabilities are determined from the equations and the cross-link density of the epoxy-rich system can be determined as below.

The cross-link density for the epoxy-rich system is the sum of the concentrations of cross-link points formed by the epoxy/amine and etherification reactions. However, there may be a change in slope of the T_g vs. conversion relationship at the conversion of 0.8 for the excess epoxy system, corresponding to the change in the dominating chemical reaction, from the epoxy/amine reactions to the etherification reaction (see later), because the cross-link points formed by the two reactions differ: Epoxy plus secondary amine, both in the gel, will generally form two trifunctional nitrogen-centered cross-link points,[36] whereas the subsequent etherification reaction of epoxy plus hydroxyl, both in the gel, will generally form one trifunctional nitrogen-centered cross-link point and one trifunctional carbon-centered cross-link point. Only one carbon atom separates the nitrogen- and carbon-centered cross-link sites, resulting in the two trifunctional cross-links being equivalent to one tetrafunctional cross-link originating from a single point. It is considered that a tetrafunctional cross-link originating from a single point may not be much more effective at raising T_g than a trifunctional cross-link point originating from a single point, especially in this case where the fourth arm is more flexible due to the oxygen linkage than are the other three. In contrast, the tetrafunctional diamine used in this work is considered to produce two trifunctional cross-link points[3,4,36] because the distance between the two amine groups is on the order of the length of epoxy segments. Hence, only one of the two cross-link points added by the etherification reaction, the nitrogen-centered cross-link site, may have a significant effect on T_g. For the epoxy-rich system, two cases are considered in calculating the effective cross-link density used in eq. (6). First, the effective cross-link density is considered to be due to only nitrogen-centered cross-links as calculated by eq. (7), whereas in the second case, both nitrogen and carbon-centered cross-link points are considered to be equally effective and the cross-link density is determined from the following equation:

$$X = \frac{a_{10}}{2}(4P(F_A^{out})[1 - P(F_A^{out})]^3 + 2[1 - P(F_A^{out})]^4) + e_0 x_{B,C}[1 - P(F_B^{out})] \times [1 - P(F_B^{in})](1 - P(F_C^{out})P(F_B^{out})) \quad [15]$$

The constants in the T_g vs. conversion relationship [eq. (6)] are determined as follows. Assuming that k is proportional to e_0, k is found to be $0.00175e_0$ from a plot of $(1/T_{g0} - 1/T_g)/e_0$ vs. x in the pregel region (where $X = 0$ and $T_g = T_{gu}$) using data from all three stoichiometries.[28] The values of the constants K and Ψ used in the theoretical equation are taken as 0.24 and 0.0, respectively, being found by forcing the equation through $T_{g\infty}$ for the amine-rich and 1 : 1 stoichiometric systems and through $T_{g\infty 1}$ of the epoxy-rich system.[28] Similar values were also obtained by plotting

$$\frac{X}{1 - \dfrac{1/T_g}{1/T_g - kx}}$$

vs. X^2 for both off-stoichiometric and 1 : 1 systems, although the scatter in the data was high.[28]

The fit of the T_g vs. conversion relationship [eq. (6)] for the amine-rich system is shown in Figure 5. For the epoxy-rich system, two calculated curves are plotted in Figure 6: One in which only nitrogen-centered cross-links are considered effective, and the other in which all trifunctional cross-links are considered to be equally effective. The experimental $T_{g\infty 2}$ of the epoxy-rich system is somewhat better predicted by the former case. Thus, the T_g vs. conversion relationship used later in this work for the epoxy-rich system will be that considering only nitrogen-centered cross-links as effective. For the 1 :

1 data,[3,4] T_g is overpredicted by approximately 10°C or less above conversions of 0.8.[28]

It should be noted that the above analysis assumes that 100% conversion of the epoxy is obtained. In fact, other researchers have found by Fourier transform infrared spectrometry (FTIR) that in this particular and other 1 : 1 epoxy/amine systems 4–8% epoxy is unreacted at "full" conversion due to topological constraints.[41-43] However, since FTIR data are generally reliable to only ±5% and since the levels of unreacted epoxy in the off-stoichiometric systems should be lower than in the 1 : 1 system (due to the excess amine in the amine-rich system and to the high concentration of hydroxyl coupled with the increased flexibility of segments in the epoxy-rich system), it is assumed that full conversion is achieved for the off-stoichiometric systems.

The calculated T_g vs. conversion relationships will be used later to transform experimental T_g to conversion for kinetic analysis of the data, and they will also be used to transform the conversion calculated from the kinetic model to T_g in order to compare calculated and experimental results. For the epoxy-rich system, the T_g vs. conversion relationship obtained by considering that only nitrogen-centered cross-links are effective will be used.

Time–Temperature Superposition of DSC Data

Time–temperature shifts of T_g vs. log time data at different cure temperatures yield a master curve for the reaction at an arbitrary reference temperature.[3,4] The theoretical basis for the superposition is the one-to-one relationship between conversion and T_g, and the assumption that the polymerization is kinetically controlled with a single apparent activation energy. The apparent activation energy obtained will correspond to the activation energy for the reactions of epoxy with primary and secondary amine if the etherification reaction is insignificant in the early stages of reaction and the activation energies of the epoxy/amine reactions are the same ($\alpha = k_2/k_1$ = constant); the apparent activation energy obtained will correspond to the activation energies for all competing reactions (etherification and the epoxy/amine reactions) if all activation energies are the same. In the latter case, which is found in this work, the data will superpose throughout the entire curing process although they are shifted to superpose only at low conversions.

For the time–temperature superposition, no knowledge of the form of the rate expression with respect to epoxide conversion, x, is necessary.[3,4,44] The rate of a kinetically controlled reaction is given by the Arrhenius rate expression:

$$\frac{dx}{dt} = k_0 \exp\left(\frac{-E_a}{RT_c}\right) f(x) \qquad (16)$$

where k_0 is the Arrhenius front factor, E_a is the apparent activation energy for the overall reaction, T_c is the cure temperature, and $f(x)$ is assumed to be a function of x independent of temperature. From the kinetic model (see later) and for the case where all competing reactions have the same activation energy, $f(x)$ will be a complex function of the epoxide conversion, x: $f(x) = (1 - x)(x + b)(1 - x_1 + \alpha x_2) + \beta(1 - x)x$, where x_1 is the conversion of primary amine, x_2 is the yield of secondary amine, and b, α, and β are constants. In contrast, $f(x)$ is a function of temperature in other work on a dicyanate ester/polycyanurate system.[28,45] Rearranging eq. (16) and integrating yields,

$$\ln \int_0^x \frac{dx}{f(x)} = \ln k_0 + \ln t - \left(\frac{E_a}{RT_c}\right) \qquad (17)$$

Since the left-hand side of the equation is only a function of conversion, and because there is a one-to-one relationship between conversion and T_g, some function of T_g, $F(T_g)$, can be substituted for the left-hand side of the equation:

$$F(T_g) = \ln k_0 + \ln t - \left(\frac{E_a}{RT_c}\right) \qquad (18)$$

The shift factor, $A(T)$, is the ln time difference at constant T_g (i.e., constant conversion) between the T_g vs. ln time curve for cure temperature T_c and the curve for an arbitrary reference temperature T_r:

$$A(T) = \ln t_r - \ln t = \left(\frac{-E_a}{R}\right)\left(\frac{1}{T_c} - \frac{1}{T_r}\right) \qquad (19)$$

The T_g vs. ln time data are time–temperature shifted horizontally to form a master curve at low conversion (to insure that the shift is in the kinetically controlled epoxy/amine reaction region), at an arbitrary reference cure temperature of 150°C for each off-stoichiometric ratio as shown in Figures 7 and 8. The master curve for the 1 : 1 stoichiometry at 140°C is shown in Figure 9 for comparison.[3,4] The data branch off of the kinetically controlled master curve at the onset of diffusion control, which ap-

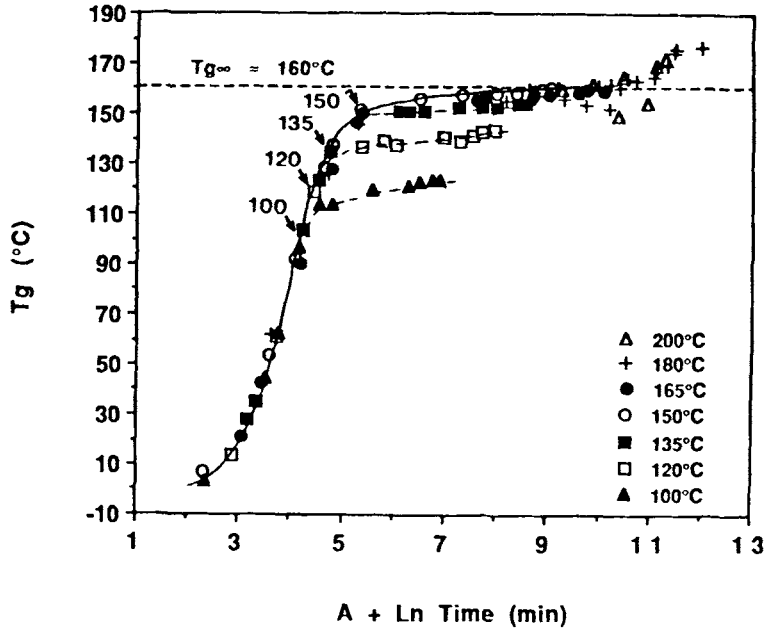

Figure 7 T_g vs. ln time master curve for the amine-rich system at 150°C. Isothermal vitrification at $T_g = T_c$ is designated by arrows. The master curve is designated by the full line. Diffusion control causes deviations from the master curve after vitrification, as shown by the dashed lines.

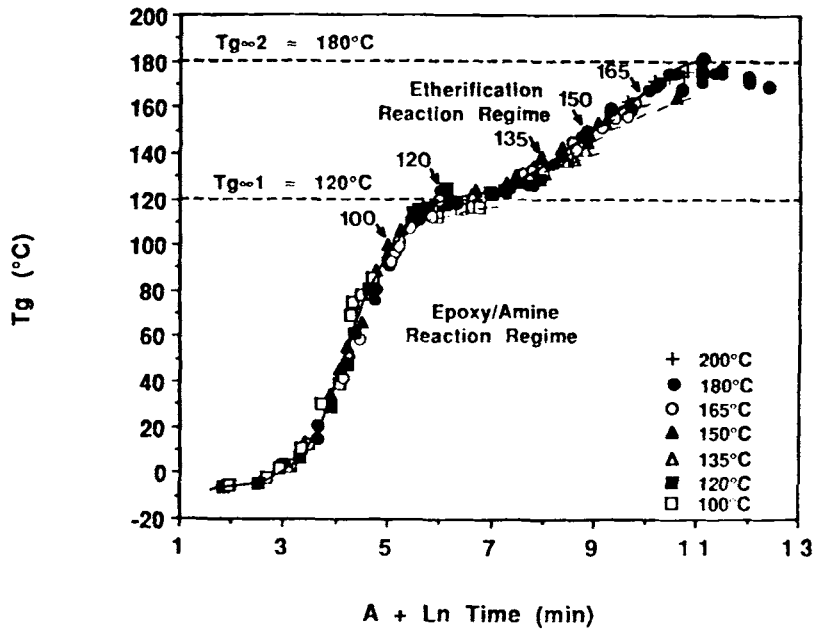

Figure 8 T_g vs. ln time master curve for the epoxy-rich system at 150°C. Data below $T_{g\infty 1}$ = 120°C fall in the epoxy/amine reaction regime, whereas data above $T_{g\infty 1}$ fall in the etherification reaction regime. Isothermal vitrification at $T_g = T_c$ is designated by arrows. The master curve is designated by the full line. Diffusion control causes slight deviations from the master curve after vitrification, as shown by the dashed lines.

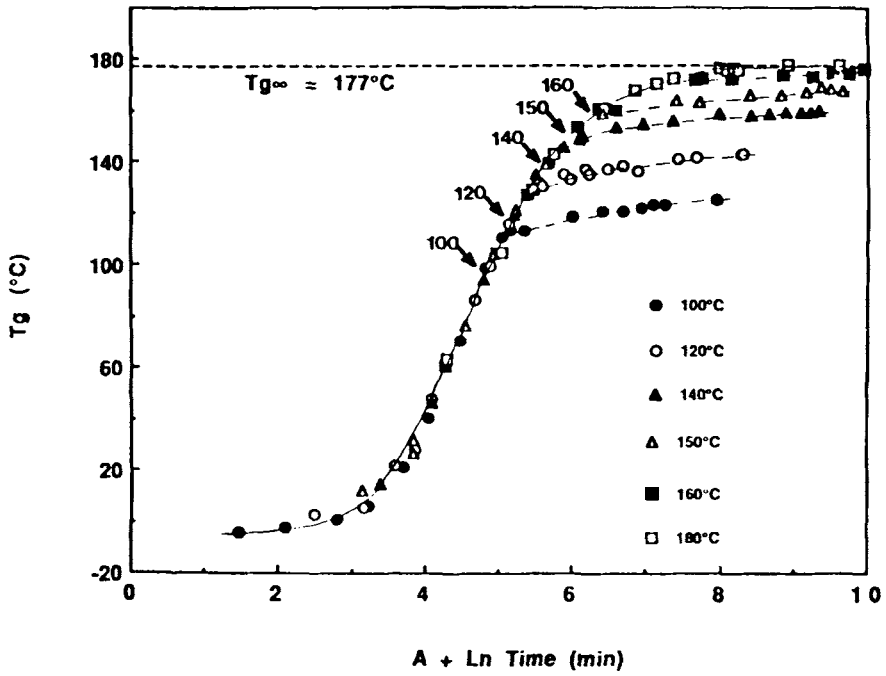

Figure 9 T_g vs. ln time master curve for the 1 : 1 stoichiometry at 140°C. Isothermal vitrification at $T_g = T_c$ is designated by arrows. Diffusion control causes deviation from the master curve after vitrification. Isothermal vitrification at $T_g = T_c$ is designated by arrows. The master curve is designated by the full line. (From [3, 4].)

proximately corresponds to vitrification (defined as $T_g = T_c$ and marked with arrows on the diagrams). Actually, diffusion control occurs when T_g is approximately 10–20°C higher than the cure temperature.

For the amine-rich and 1 : 1 systems in Figures 7 and 9, T_g levels off at long times at high cure temperatures in the absence of degradation due to completion of the epoxy/amine reactions. The ultimate T_g of the "fully" cured epoxy/amine network, $T_{g\infty}$, is approximately 160 and 177°C for the excess amine and 1 : 1 systems, respectively. For the excess epoxy system in Figure 8, the plateau observed at 120°C also corresponds to completion of the epoxy/amine reactions and to $T_{g\infty 1}$ of the epoxy-rich system. There is no residual heat observed in the epoxy/amine exotherm region of the DSC scans for $T_g = T_{g\infty}$ in the amine-rich and 1 : 1 systems or for $T_g > T_{g\infty 1}$ in the epoxy-rich case. $T_{g\infty}$ for the amine-rich system is less than that of the 1 : 1 system because its cross-link density is lower. For the epoxy-rich system, $T_{g\infty 1}$ is lower not only because of decreased cross-link density but also because of plasticization by the excess epoxy chain ends.

At cure temperatures below $T_{g\infty}$, reactions become diffusion-controlled after isothermal vitrification ($T_g = T_c$, designated by arrows in the figures) due to the decreased mobility below T_g, and also at high conversion due to increasing distance between reactive sites. Diffusion control is observed when data branch off from the master curve due to the progressively increasing time scale of diffusion. In the glassy and/or high conversion limits, the time for diffusion of reacting species is much longer than the time for their kinetically controlled chemical reaction; hence, the rate is controlled only by the diffusion of reactive groups.

In the amine-rich system, the data of Figure 7 are inconsistent at long times for cure temperatures of 180 and 200°C (A + ln time $\gtrsim$ 10; i.e., $\gtrsim$ 15 days). It is considered that this inconsistency is due to inadvertent degradation reactions, with one degradation reaction decreasing T_g, perhaps due to thermal degradation in the absence of oxygen,[46] whereas another degradation reaction increases T_g possibly in the presence of oxygen (for example, if the DSC pan were not sealed properly).

There are two $T_{g\infty}$'s associated with the epoxy-rich system, as shown in Figure 8. $T_{g\infty 1}$ corresponds to depletion of amine and completion of the epoxy/

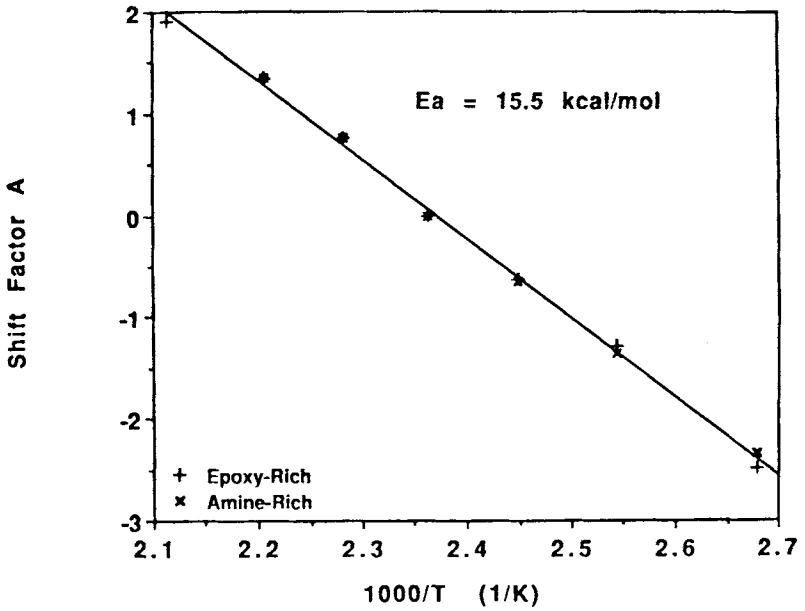

Figure 10 Arrhenius plot of shift factor, $A(T)$, vs. reciprocal cure temperature $(1/K)$ for the epoxy/amine reaction region with data from both the amine and epoxy-rich systems. The slope yields the apparent activation energy.

amine reactions as previously discussed, whereas $T_{g\infty 2}$ is due to "full" conversion of the epoxy presumably by etherification. $T_{g\infty 2}$ is approximately 180°C, approximately the same as $T_{g\infty 1}$ of the 1 : 1 system (177°C). The residual isothermal exotherm measured at 320°C, which reflects the excess epoxy present in the system, decreases to zero as T_g approaches $T_{g\infty 2}$. However, the increased scatter in the data of Figure 8 at long times, $A + \ln \text{time} \gtrsim 10$, indicates that the etherification reaction may be complicated by degradation reactions similar to those encountered in the amine-rich system at long times. It is assumed, however, that since the data for cure temperatures of 180 and 200°C time–temperature superpose that degradation does not significantly affect the value found for $T_{g\infty 2}$. (It is expected that the activation energy for degradation reactions would be higher than that for the curing reactions, and that if degradation were significant, the data would not superpose.)

The apparent activation energy of the reactions is determined from eq. (19). Plotting the shift factors used to form the master curves for both excess amine and excess epoxy stoichiometries against reciprocal cure temperature $(1/K)$ yields a straight line with a slope $-E_a/R$, as shown in Figure 10, where E_a is the apparent activation energy for the epoxy/amine polymerization and R is the gas constant. The apparent activation energy, thus obtained, is 15.5 kcal/mol (63.1 kJ/mol), compared with the activation energy of 15.2 found for the 1 : 1 mixture.[3,4] The value of 15.5 kcal/mol is used in calculations in this work.

Although the epoxy-rich master curve was obtained by shifting at low conversions in the epoxy/amine reaction regime, the data at high T_g's (high conversions), in the etherification reaction region, also superpose as shown in Figure 8. This implies that the activation energy for the etherification reaction is similar to that of the epoxy/amine reactions at 15.5 kcal/mol. Other work in the literature using a commercial aromatic epoxy resin cured with a mixture of dicyandiamide and diuron amine, in a 1 : 0.24 epoxy : amine stoichiometric ratio, also concluded that the activation energies for the epoxy/amine and epoxy/hydroxyl reactions were similar (at 20.3 kcal/mol).[47] It is observed that in the etherification reaction region diffusion-control also occurs at vitrification, as marked by the arrows in Figure 8, but its effect is much less apparent than in the epoxy/amine reaction regime due to the slower rate of the etherification reaction.

Kinetic Model of the Curing Reactions

The 1 : 1 stoichiometric reaction of DER332 with TMAB has been shown to be satisfactorily described by a second-order mechanism for the epoxy/amine

reactions autocatalyzed by hydroxyl groups generated during the reaction, with an apparent activation energy of 15.2 kcal/mol and assuming equal reactivities of amino hydrogens.[3,4] A similar model is used in this work to describe the off-stoichiometric systems but with the added complexity of the etherification (epoxy/hydroxyl) reaction and a consideration of unequal reactivities of amino hydrogens. The reactions considered are the epoxy/amine reactions, catalyzed by the hydroxyl generated by the reaction (OH) or by initial hydroxyl or impurities (HX_0) as other researchers have proposed,[48] and the etherification reaction:

$$E + A1 \xrightarrow[k_{10}]{OH} A2$$

$$E + A1 \xrightarrow[k'_{10}]{HX_0} A2$$

$$E + A2 \xrightarrow[k_{20}]{OH} A3$$

$$E + A2 \xrightarrow[k'_{20}]{HX_0} A3$$

$$E + OH \xrightarrow[k_{30}]{} Et + OH$$

where E, A1, A2, A3, OH, and Et designate epoxy, primary amine, secondary amine, tertiary amine, hydroxyl, and ether species, respectively. The equations catalyzed by hydroxyl or impurities (HX_0) are particularly significant in the absence of hydroxyls generated during the reaction. Etherification is assumed to be first order with respect to both epoxy and hydroxyl concentrations. The reaction is not considered to be catalyzed by tertiary amine due to steric hindrance, although if it were the concentration of tertiary amine could be incorporated into k_{30} since it is constant when the etherification reaction is significant.

The change with time of epoxide and primary amine fractional conversions, x and x_1, and fractional yield of secondary amine, x_2, can be described by the following differential equations:

$$\frac{dx}{dt} = k_1(1-x)(x+b)(1-x_1+\alpha x_2) + k_3(1-x)x \quad (20)$$

$$\frac{dx_1}{dt} = k_1 r(1-x)(x+b)(1-x_1) \quad (21)$$

$$\frac{dx_2}{dt} = k_1 r(1-x)(x+b)(1-x_1-\alpha x_2) \quad (22)$$

The normalized rate constants for the reaction of epoxy with primary amine is k_1 ($= k_{10}e_0a_{10}$, where e_0 is the initial concentration of epoxy and a_{10} is the initial concentration of primary amine), for epoxy with secondary amine is k_2 ($= k_{20}e_0a_{10}$), and for the etherification reaction is k_3 ($= k_{30}e_0$). The dimensionless ratio of the rate constants for the reactions of epoxy with secondary and primary amine groups is $\alpha = k_2/k_1$, and for the reactions of epoxy with hydroxyl and primary amine groups is $\beta = k_3/k_1$. The stoichiometric ratio, r, is e_0/a_{10}. The constant b is considered to be the concentration of hydroxyl impurities that catalyze the reaction, which is particularly significant in the absence of hydroxyls generated by the reaction.[48] Some researchers alternatively assume that there are uncatalyzed mechanisms for the reactions of epoxy with primary and secondary amino hydrogens, rather than the reactions catalyzed by impurity OH_0, and then b is interpreted as the ratio of the rate constants for uncatalyzed and hydroxyl-catalyzed reactions.[14] The latter interpretation would be expected to give a temperature-dependent value, with b increasing with increasing temperature assuming that the uncatalyzed reaction has a higher activation energy. In this work, it is assumed that b is constant and $k'_{10} = k_{10}$ and $k'_{20} = k_{20}$ in order to make the model less cumbersome. It should be noted that the effect of volume changes during cure on the rate constants is not considered here.

To use the above model of the reaction, several parameters must be determined from the experimental data. The values of k_1, b, α, and β need to be determined at a reference temperature (150°C). The values of the Arrhenius activation energies for the reaction of epoxy with primary amine, secondary amine, and hydroxyl are also needed.

The values of the rate constant for the reaction of epoxy with primary amine, k_1, and the constant b are determined during the early stages of the epoxy/amine reactions, where it is assumed that no etherification occurs. Equation (20) can be rewritten in the following form, assuming that the epoxy/hydroxyl reaction is insignificant:

$$\frac{\dfrac{dx}{dt}}{e_0a_{10}(1-x)(1-x_1+\alpha x_2)} = k_{10}(x+b) \quad (23)$$

The rate dx/dt is determined from polynomial fits of the master curve x vs. ln time data (from Figs. 7 and 8). The constant α at the master curve reference temperature of 150°C is assumed to be in one case 0.5, the value for equal reactivity of amino hydrogens that was assumed in earlier work in our laboratory

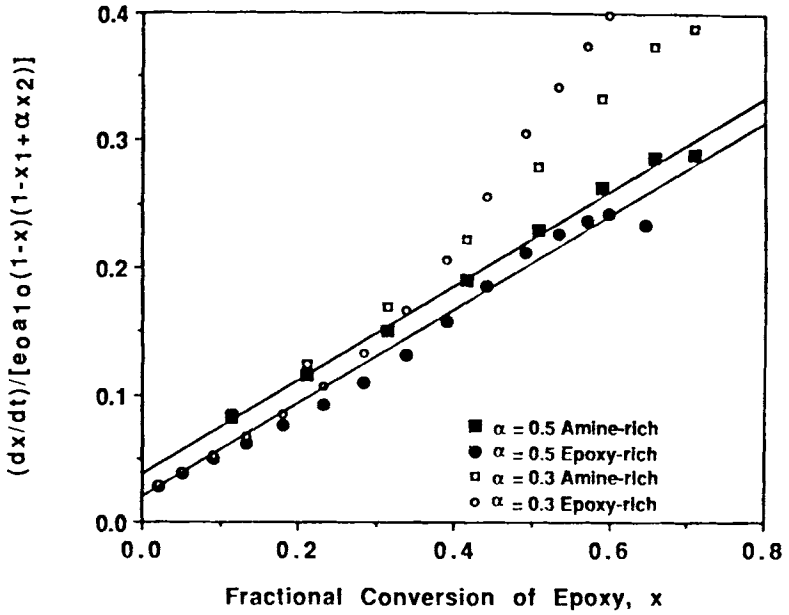

Figure 11 Determination of kinetic parameters for epoxy/amine reactions for the amine-rich and epoxy-rich systems. For the correct value of α, the slope of the line for both systems will yield the same normalized rate constant. The constant b is determined from the y-intercept of the lines.

when modeling the kinetics of the 1 : 1 stoichiometric ratio of the system, and in a second case, it is assumed to be 0.3 as found in FTIR work in our laboratory on the 1 : 1 system at 150°C.[9] The values of x_1 and x_2 are determined, as a function of x and α, from the following relations, the first based on the stoichiometric reaction relationship neglecting etherification (as is appropriate at low conversions) and the second derived by dividing eq. (22) by eq. (21) and integrating:

$$x = \frac{1}{r}(2x_1 - x_2) \tag{24}$$

$$x_2 = \frac{1}{1-\alpha}[(1-x_1)^{\alpha} - (1-x_1)] \tag{25}$$

Plotting the left-hand side of eq. (23) vs. x should yield, for the correct value of α, a straight line with a slope of k_{10} and a y-intercept of $k_{10}b$. Figure 11 shows plots for both $\alpha = 0.3$ and 0.5. The value of k_{10} is expected to be the same for systems of different stoichiometry. It is therefore concluded that the value of α is approximately 0.5, since for this case, a straight line is obtained with a slope, $k_{10} = 0.37$ min^{-1} (150°C), independent of stoichiometry for the two cases. The constant b is determined from the fit of the data for $\alpha = 0.5$ to be 0.10 and 0.05 for the amine-rich and epoxy-rich systems, respectively. More prereaction in preparing the amine-rich formulation would account for the different values of b.

The apparent activation energy in the epoxy/amine reaction regime and for the etherification reaction was previously determined to be 15.5 kcal/mol from the time–temperature superposition of the T_g vs. ln time data. Since the kinetic ratio α is approximately 0.5, this apparent activation energy is also the activation energy for the reaction of epoxy with primary amine and for the reaction of epoxy with secondary amine. From the time–temperature shift, it was found that data in the etherification reaction regime also superposed, and, consequently, the activation energy for that reaction is also considered to be 15.5 kcal/mol.

Assuming that the other parameters are correct, the calculation with β ($= k_3/k_1$) equal to 0.001 is found to satisfactorily describe the master curve data at 150°C throughout the kinetically controlled reaction, including the epoxy/hydroxyl reaction regime, i.e., for $x > 0.8$ in the epoxy-rich system.[28] This value is an order of magnitude lower than that found by other researchers investigating similar systems.[14] However, this is considered to be due to the difference in the reactions considered. The other

researchers considered that b was a function of temperature so that there were two epoxy/amine reactions considered, one uncatalyzed and the other catalyzed by hydroxyl, and they considered that the etherification reaction could also be either uncatalyzed or catalyzed by hydroxyl. The ratios that are reported in their work are the ratio of the uncatalyzed etherification rate constant to the uncatalyzed epoxy/amine rate constant and the ratio of the catalyzed etherification rate constant to the catalyzed epoxy/amine rate constant. In contrast, in this work, the etherification reaction is considered to be uncatalyzed and the epoxy/amine reactions are considered to be catalyzed by hydroxyl. The ratio of the other researchers' uncatalyzed etherification rate constant to their hydroxyl-catalyzed epoxy/amine rate constant varies from 0.0004 to 0.002 with temperature for two different amines and compares favorably to the value obtained in this work.

Diffusion control becomes important for the epoxy/amine reactions in the vicinity of vitrification, $T_g = T_c$. This is demonstrated by the deviation of data from the kinetically controlled master curves in Figures 7–9. Similar to other work in this area,[3,4,20,21] diffusion control in this work is accounted for by assuming that the time for the disappearance of a reactant is equal to the time for diffusion plus the time for chemical reaction. The normalized rate constants are thus

$$\frac{1}{k_i} = \frac{1}{k_{i,c}} + \frac{1}{k_{i,d}} \tag{26}$$

where k_i is the observed normalized rate constant, where subscript $i = 1$ refers to the reaction of epoxy with primary amine and $i = 3$ refers to the etherification reaction, $k_{i,c}$ is the rate constant in the kinetically controlled regime ($k_{1,c} = 0.37 e_0 a_{10}$ and $k_{3,c} = 0.00014 e_0$ at 150°C for $\alpha = 0.5$), and $1/k_{i,d}$ is the time scale for diffusion, which is considered to depend not only on the mobility but also on the average diffusion length scale for each particular reaction (i.e., $k_d \propto D/\lambda$, where D is the diffusivity and λ is the length of diffusion). Thus, different reactions may have different time scales of diffusion depending on the proximity and the mobility of reacting groups.

Although the free-volume-based Doolittle[23] and WLF equations[22] are inadequate for describing the glassy state compared to the nonequilibrium equation of Adam and Gibbs,[21] they have been used because of their relative simplicity to satisfactorily describe the diffusion-controlled kinetics in similar work.[3,4,20] The major criticism of the free-volume equations is that only the free volume, and not temperature, is considered to determine the properties of a material below T_g,[21] which is compensated for by the activation energy term in the Macedo and Litovitz equation.[25] However, due to its simplicity and the satisfactory results, the Doolittle free-volume equation[23] will be used here to model the diffusion-controlled kinetics:

$$k_d = A \exp\left(\frac{-b}{f}\right) \tag{27}$$

where A and b are taken as adjustable parameters and f is the fractional free volume. Note that the effect of changing diffusion length with conversion is not explicitly incorporated. The fractional free volume, f, in this work is assumed to be the equilibrium value as calculated using the "universal" values found for linear polymers from the WLF equation (i.e., the linear expansivity of free volume above T_g is $0.00048°C^{-1}$ and the fractional free volume at T_g is 2.5%). The equilibrium fractional free volume is extrapolated to below T_g:

$$f = (T_c - T_g)(4.8e^{-4}) + 0.025 \tag{28}$$

The decrease in the mobility in the glass transition region, from above to approximately 20°C below T_g, is qualitatively described by the Doolittle and WLF equations used. It is noted that the modified WLF equation, used to model diffusion in other work in this laboratory,[3,4] is qualitatively more correct in the glassy state since it predicts that the molecular mobility in the glassy state below the glass transition region decreases slowly rather than exponentially with decreasing temperature.[28] However, since T_g never rises more than 25°C above the curing temperature for the time scales studied, and since the decrease in mobility is over 10-fold over the glass transition region prior to the deviation of the modified WLF and WLF equations, there is no advantage in this work of using the modified WLF equation over the WLF or Doolittle free-volume equations. In contrast, one advantage of the free-volume equation is that since the fractional free volume is explicit the effects of physical aging after vitrification can be accounted for in future work, by allowing the fractional free volume to be time-dependent when the material is in the glassy state, $T_g > T_c$.

The values of A and b in eq. (27) for both epoxy/amine and etherification reaction regimes are determined from plots of ln k_d [determined from eq. (26)] vs. $1/f$ [determined from eq. (28)] from data

in the diffusion-controlled region of the amine-rich and epoxy-rich systems, respectively. The parameters are found to be 100 and 0.2 (at 135°C) for the epoxy/amine reactions (k_1) in the amine-rich system and 0.4 and 0.2 (using limited data from all cure temperatures) for the etherification reaction (k_3) in the epoxy-rich system.[28] Although there is an indication that A and b vary with temperature for the epoxy/amine reactions, as might be expected, it is not necessary to assume an activated diffusion process in order to satisfactorily describe the data. The difference in the values of A for the two reactions may reflect only the difference in mobility between the two systems when diffusion control becomes significant, with the amine-rich system having more mobility due to its decreased cross-link density.

Equations (20) and (21) can now be solved numerically using the Runge–Kutta technique to yield conversion as a function of time throughout the entire range of cure, including the diffusion-controlled regime. Conversion is then transformed to T_g by using the theoretical curve that fits the experimental T_g vs. conversion data. Figures 12 and 13 compare the experimental and calculated T_g vs. ln time curves for excess amine and excess epoxy stoichiometries, respectively. (Note that data points after the onset of degradation at long times for cure temperatures of 180 and 200°C are not plotted for the amine-rich system for simplicity.)

It is apparent from comparison of the calculations with the experimental data that the data can be fit adequately by the calculations with α equal to 0.5. Data in the etherification regime of the epoxy-rich system are also fit well by the calculation. This supports the conclusion that the activation energies for the epoxy/amine and etherification reactions are approximately the same. Further, the experimental data for the 1 : 1 stoichiometric system[3,4] are also satisfactorily described by the model,[28] indicating that the model should be able to predict other stoichiometries as well. The reaction model is useful for predicting not only conversion as a function of cure time and temperature, but also for optimizing processing conditions and final properties for various processes. Gelation and/or vitrification can be used to control exotherms,[1] rheology,[49] density,[26] dimensional stability,[1,50] etc.

Calculation of Time–Temperature–Transformation (TTT) Isothermal Cure Diagrams

A complete set of iso-T_g contours prior to the onset of diffusion control (which occurs after vitrification) and the vitrification contour ($T_g = T_c$) of the TTT isothermal cure diagram can be calculated using the kinetically controlled master curve, which describes the reaction from T_{g0} to $T_{g\infty}$, and using the apparent activation energy obtained from the time–temper-

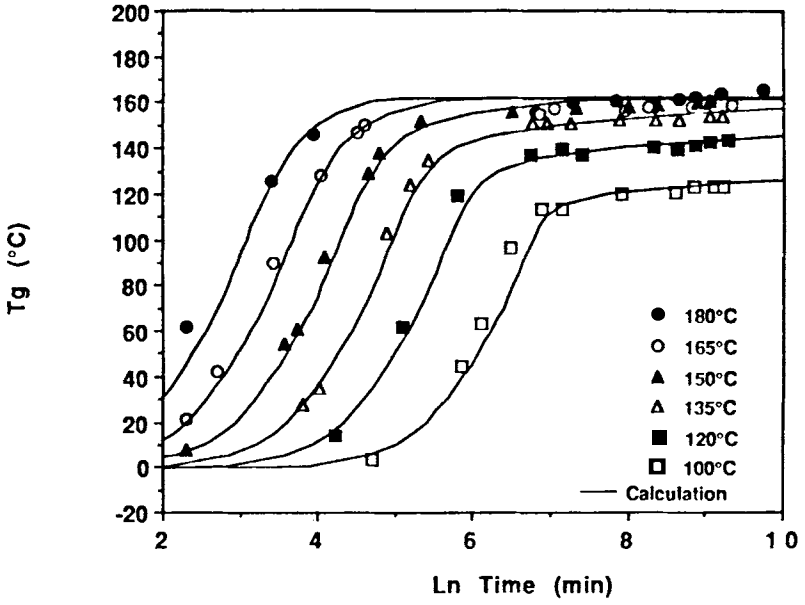

Figure 12 T_g vs. ln time data for amine-rich system: (solid line) calculation using amine-rich parameters; (symbols) experimental data.

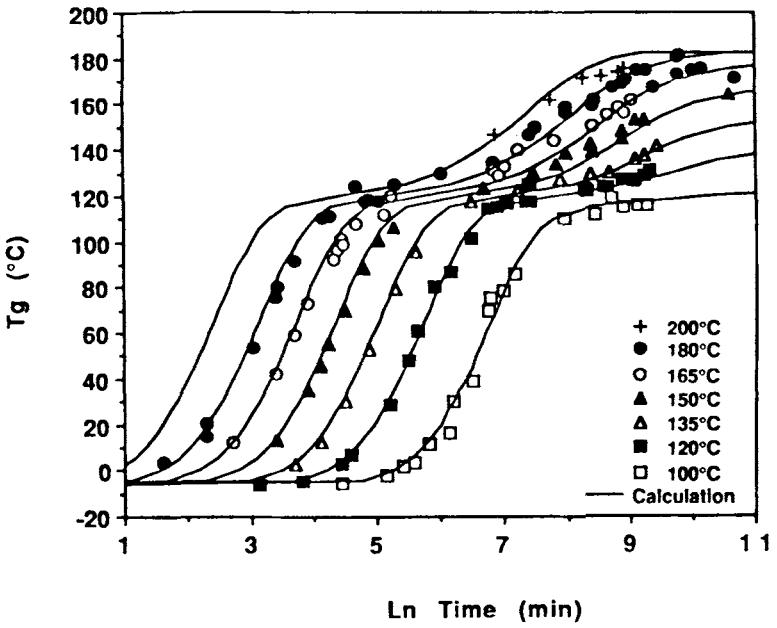

Figure 13 T_g vs. ln time data for epoxy-rich system: (solid line) calculation using epoxy-rich parameters; (symbols) experimental data.

ature superposition in eq. (19). However, iso-T_g contours cannot be extended into the diffusion-controlled regime by this method since the master curve used is only valid for the kinetically controlled regime. Consequently, more complete TTT diagrams are calculated from the reaction model.

Figures 14 and 15 show plots of the calculated TTT diagrams for the two off-stoichiometric systems with iso-T_g and vitrification contours. The iso-T_g curves are calculated throughout cure, even after vitrification, using the reaction model. As expected, there is a noticeable difference in the shapes of the vitrification curves for the two off-stoichiometric systems. The vitrification curve of the amine-rich sample levels off at cure temperatures close to $T_{g\infty}$ as expected, due to full conversion of the epoxy. The vitrification curve for the excess epoxy sample, however, begins to level off at $T_{g\infty 1}$ for the 1 : 0.8 epoxy/amine network, but then increases again and levels off at $T_{g\infty 2}$ for the fully converted material.

The dotted lines show calculated degradation/devitrification contours obtained from the master curve, which are calculated assuming that the activation energy for degradation reactions is the same as for the curing reactions, which is not expected to be the case. However, there were not enough data at different reaction temperatures in the degradation regime to determine the activation energy(ies) or reaction kinetics of the degradation reaction(s).

CONCLUSIONS

In summary, the cure of excess amine and excess epoxy DER332/TMAB systems has been studied. A one-to-one relationship between T_g and conversion is found for the epoxy/amine reaction regimes for both systems and is described by a theoretical equation. T_g is thus used as the principal parameter for monitoring the reaction. From the single apparent activation energy for the overall reactions, and the shape of the master and vitrification curves, it is concluded that the epoxy/hydroxyl reaction becomes significant in the excess epoxy sample only after the amine concentration is nearly depleted. The epoxy/amine reactions for the both stoichiometric systems, and the etherification reaction in the excess epoxy system, are satisfactorily described throughout the entire cure process, including the diffusion-controlled regime, by a reaction model of the epoxy/amine and epoxy/hydroxyl reactions. The ratio of the rate constants for reaction of epoxy with secondary and primary amine, respectively, $\alpha = k_2/k_1$, is found to be independent of temperature and equal to 0.5. The ratio of the rate constants for the epoxy/hydroxyl and epoxy/primary amine reaction, $\beta = k_3/k_1 = 0.001$. Iso-T_g and vitrification contours on the TTT isothermal cure diagrams are calculated for each system from the reaction model.

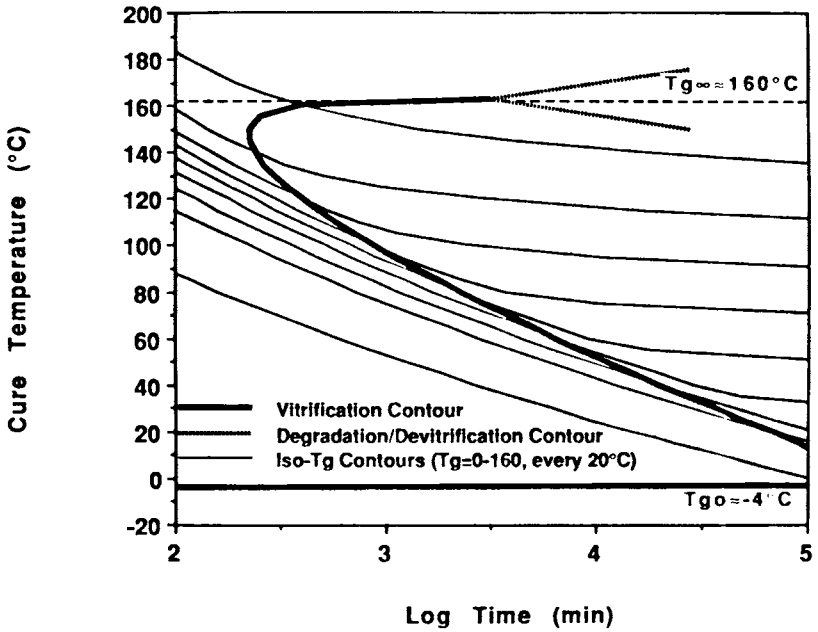

Figure 14 Calculated TTT isothermal cure diagram for the amine-rich system with vitrification and iso-T_g contours from kinetic model. Degradation/devitrification contours are dotted and are calculated from the kinetically controlled master curve assuming that the curing and degradation reactions have similar activation energies.

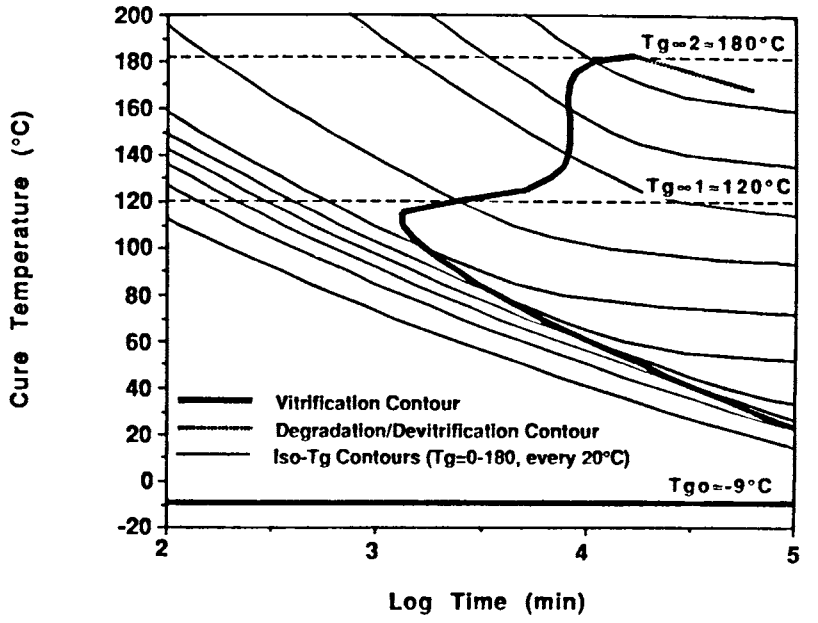

Figure 15 Calculated TTT isothermal cure diagram for the epoxy-rich system with vitrification and iso-T_g contours from kinetic model. Degradation/devitrification contours are dotted and are calculated from the kinetically controlled master curve assuming that the curing and degradation reactions have similar activation energies.

PARTIAL LIST OF SYMBOLS

A	Parameter in Doolittle free-volume equation
$A(T)$	Shift factor between two T_g vs. ln time curves at different cure temperatures
b	Initial concentration of hydroxyl; also parameter in Doolittle free-volume equation
E_a	Apparent activation energy for overall epoxy/amine reaction
f	Free-volume fraction
k	Parameter in T_g vs. conversion equation incorporating effect of dangling chains on T_g; also, overall rate constant in epoxy/amine system
k_1	Rate constant for reaction of epoxy with primary amine (t^{-1})
k_2	Rate constant for reaction of epoxy with secondary amine (t^{-1})
k_3	Rate constant for reaction of epoxy with hydroxyl (t^{-1})
K	Parameter in eq. (6) incorporating effect of cross-links on T_g
$P(F_A^{in})$	Probability of finding a finite, rather than infinite, chain looking into A
$P(F_A^{out})$	Probability of finding a finite, rather than infinite, chain looking out from A
$P(F_B^{in})$	Probability of finding a finite, rather than infinite, chain looking into B
$P(F_B^{out})$	Probability of finding a finite, rather than infinite, chain looking out from B
$P(F_C^{in})$	Probability of finding a finite, rather than infinite, chain looking into C
$P(F_C^{out})$	Probability of finding a finite, rather than infinite, chain looking out from C
R	Gas constant
t	Isothermal cure time
t_r	Reference isothermal cure time
T_c	Isothermal cure temperature
T_g	Glass transition temperature
T_{g0}	Glass transition temperature of uncured material
$T_{g\infty}$	Glass transition temperature of fully cured material
$T_{g\infty 1}$	Glass transition temperature of the fully developed epoxy/amine network in epoxy-rich material
$T_{g\infty 2}$	Glass transition temperature of epoxy/amine + epoxy/hydroxyl networks in the fully developed epoxy-rich material
T_r	Reference isothermal cure temperature
x	Fractional conversion of epoxy in epoxy/amine reaction
x_1	Fractional conversion of primary amine
x_2	Yield of secondary amine
x_3	Yield of tertiary amine
x_A	Fractional conversion of amino hydrogen
x_B	Fractional conversion of epoxy
x_C	Fractional conversion of epoxy due to etherification
α	k_2/k_1
β	k_3/k_1
ΔH_r	Residual heat of DSC exotherm; subscripts 1 and 2 refer to epoxy/amine and excess epoxy exotherms, respectively
ΔH_T	Total heat of DSC exotherm for uncured material; subscripts 1 and 2 refer to epoxy/amine and excess epoxy exotherms in the epoxy/amine system, respectively
Ψ	Parameter in T_g versus conversion relation incorporating effect of non-Gaussian nature of cross-links at high cross-link density on T_g

REFERENCES

1. J. K. Gillham, *Polym. Eng. Sci.*, **26**(20), 1429 (1986).
2. J. B. Enns and J. K. Gillham, *J. Appl. Polym. Sci.*, **28**, 2567 (1983).
3. G. Wisanrakkit, PhD Thesis, Princeton University, 1990.
4. G. Wisanrakkit and J. K. Gillham, *J. Coat. Tech.*, **62**(783), 35 (1990); *J. Appl. Polym. Sci.*, **41**, 2885 (1990).
5. Y. Tanaka and R. S. Bauer, in *Epoxy Resins: Chemistry and Technology*, C. A. May, Ed., Marcel Dekker, New York, 1988, p. 285; Y. Tanaka and T. F. Mika, in *Epoxy Resins: Chemistry and Technology*, C. A. May and Y. Tanaka, Eds., Marcel Dekker, New York, 1973, p. 135.
6. B. A. Rozenberg, *Adv. Polym. Sci.*, **78**, 113 (1986).
7. K. Dusek, *Adv. Polym. Sci.*, **78**, 1 (1986).
8. S. Lunak and K. Dusek, *J. Polym. Sci.*, **53**, 45 (1979).
9. X. Wang and J. K. Gillham, *J. Appl. Polym. Sci.*, **43**, 2267 (1991).
10. A. C. Grillet, J. Galy, J. P. Pascault, and I. Bardin, *Polymer*, **30**, 2094 (1989).
11. L. Chiao, *Macromolecules*, **23**, 1286 (1990).
12. C. S. P. Sung, E. Pyun, and H.-L. Sun, *Macromolecules*, **19**, 2922 (1986).
13. C.-S. Chern and G. W. Poehlein, *Polym. Eng. Sci.*, **27**(11), 788 (1987).

14. W. X. Zukas, N. S. Schneider, and W. J. MacKnight, *ACS Prepr. Polym. Mater. Sci. Eng.*, **49,** 588 (1983).
15. J. Charlesworth, *J. Polym. Sci. Polym. Chem.*, **18,** 621 (1980).
16. U. M. Bokare and K. S. Gandhi, *J. Polym. Sci. Polym. Chem.*, **18,** 857 (1980).
17. J. J. King and J. P. Bell, in *Epoxy Resin Chemistry,* ACS Symp. Ser. 114, R. S. Bauer, Ed., American Chemical Society, Washington, DC, 1979, pp. 225–257.
18. C. C. Riccardi and R. J. J. Williams, *J. Polym. Sci.*, **32,** 3445 (1986).
19. R. J. Morgan, in *Epoxy Resins and Composites I,* Advances in Polymer Science 72, K. Dusek, Ed., Springer-Verlag, New York, 1985, pp. 1–44.
20. W. M. Sanford and R. L. McCullough, *J. Polym. Sci. B Polym. Phys.*, **28,** 973 (1990).
21. S. Matsuoka, X. Quan, H. E. Bair, and D. J. Boyle, *Macromolecules,* **22,** 4093 (1989).
22. M. L. Williams, R. F. Landel, and J. D. Ferry, *J. Am. Chem. Soc.*, **77,** 3701 (1955).
23. A. K. Doolittle, *J. Appl. Phys.*, **22,** 1471 (1951).
24. D. H. Kaelble, *Computer Aided Design and Manufacture,* Marcel Dekker, New York, 1985, Chap. 4, pp. 113–148.
25. P. B. Macedo and T. A. Litovitz, *J. Chem. Phys.*, **42,** 245 (1969).
26. G. K. Wisanrakkit and J. K. Gillham, *J. Appl. Polym. Chem.*, **42,** 2453 (1991).
27. S. L. Simon, G. Wisanrakkit, and J. K. Gillham, *ACS Prepr., Polym. Mater. Sci. Eng.*, **61,** 799 (1989).
28. S. L. Simon, PhD Thesis, Princeton University, January, 1992.
29. Dr. David Sheih, Dow Chemical Company, Private communication.
30. L.-H. Lee, *J. Polym. Sci. A* **3,** 859 (1965).
31. J. M. Barton, in *Epoxy Resins and Composites I,* Advances in Polymer Science 72, K. Dusek, Ed., Springer-Verlag, New York, 1985, pp. 111–154.
32. A. Hale, C. W. Macosko, and H. E. Bair, *Macromolecules,* **24**(9), 2610 (1991).
33. P. Pang and J. K. Gillham, *J. Appl. Polym. Sci.*, **37,** 1969 (1989).
34. J. Mijovic and J. Wijaya, *Macromolecules,* **23,** 3671 (1990).
35. C. Feger and W. J. MacKnight, *Macromolecules,* **18,** 280 (1985).
36. X. Wang and J. K. Gillham, *ACS Prepr. Polym. Mater. Sci. Eng.*, **63** (1990); *J. Appl. Polym. Sci.*, to appear.
37. M. T. Aronhime and J. K. Gillham, *J. Coat. Tech.*, **56**(718), 35 (1984).
38. J. P. Pascault and R. J. J. Williams, *J. Polym. Sci. Part B Polym. Phys.*, **28,** 85 (1990).
39. T. G. Fox and S. Loshaek, *J. Polym. Sci.*, **15,** 371 (1955).
40. D. R. Miller and C. W. Macosko, *Macromolecules,* **9**(2), 206 (1976).
41. E. F. Oleinik, in *Epoxy Resins and Composites IV,* K. Dusek, Ed., Advances in Polymer Science 80, Springer-Verlag, New York, 1986, pp. 49–99.
42. V. A. Topolkarayev, L. A. Zhorina, L. V. Vladimirov, Al. Al. Berlin, A. N. Zelenetskii, E. V. Prut, and N. S. Yenikolapyan, *Polym. Sci. USSR,* **21,** 1823 (1979).
43. X. Wang, Princeton University, unpublished results, 1990.
44. S. Gan, J. K. Gillham, and R. B. Prime, *J. Appl. Polym. Sci.*, **37,** 803 (1989).
45. S. L. Simon and J. K. Gillham, *J. Appl. Polym. Sci.*, to appear.
46. L. Chan and J. K. Gillham, *J. Appl. Polym. Sci.*, **29,** 3307 (1984).
47. N. S. Schneider, J. F. Sprouse, G. L. Hagnauer, and J. K. Gillham, *Polym. Eng. Sci.*, **19**(4), 304, 1979.
48. K. Horie, H. Hiura, M. Sawada, I. Mita, and H. Kambe, *J. Polym. Sci. A,* **18,** 1357 (1970).
49. S. L. Simon and J. K. Gillham, *ACS Prepr., Polym. Mater. Sci. Eng.*, **67** (1992).
50. W. V. Breitigam, R. S. Bauer and C. A. May, *ACS Prepr., Polym. Chem.*, **33,** 511 (1992).

Received September 24, 1991
Accepted January 24, 1992